Examination of a Zoned Pegmatite and Host Rocks At Port Joli, Nova Scotia.

By
Dan MacDonald

In partial fulfillment of the requirements for an Honour's Degree in Geology
March 5, 1988.

Distribution License

DalSpace requires agreement to this non-exclusive distribution license before your item can appear on DalSpace.

NON-EXCLUSIVE DISTRIBUTION LICENSE

You (the author(s) or copyright owner) grant to Dalhousie University the non-exclusive right to reproduce and distribute your submission worldwide in any medium.

You agree that Dalhousie University may, without changing the content, reformat the submission for the purpose of preservation.

You also agree that Dalhousie University may keep more than one copy of this submission for purposes of security, back-up and preservation.

You agree that the submission is your original work, and that you have the right to grant the rights contained in this license. You also agree that your submission does not, to the best of your knowledge, infringe upon anyone's copyright.

If the submission contains material for which you do not hold copyright, you agree that you have obtained the unrestricted permission of the copyright owner to grant Dalhousie University the rights required by this license, and that such third-party owned material is clearly identified and acknowledged within the text or content of the submission.

If the submission is based upon work that has been sponsored or supported by an agency or organization other than Dalhousie University, you assert that you have fulfilled any right of review or other obligations required by such contract or agreement.

Dalhousie University will clearly identify your name(s) as the author(s) or owner(s) of the submission, and will not make any alteration to the content of the files that you have submitted.

If you have questions regarding this license please contact the repository manager at dalspace@dal.ca.

Grant the distribution license by signing and dating below.

_____ _____

Name of signatory Date

Table of Contents

List of Figures

Acknowledgements

I wish to thank the following people for their invaluable help in the scientific aspects of this thesis: P.Cerny, D.B.Clarke, S.Douma, G.Eberz, J.Hall, R.A.Jamieson, B.MacKay, J.Reynolds, P.T.Robinson, and M.Zentilli.

I also thank K.DesRoches and R.Kempster for their help in the field. Others who indirectly helped me through the trials of constructing this thesis include C.Macek, U.Minucci, N.Sikes, R.Hunter, and D.Stirling. I also thank Dr. and Mrs.J.C.Wickwire for their cooperation and for lending their name to the pegmatites.

Special thanks are due to S.Manson, my friend and valuable field assistant for his time, skill, and companionship.

Most importantly, I especially thank Mom and Dad for their patience, support, and love they have given me over the last few years. Without them, none of this would have been possible.

Abstract

The Wickwire pegmatites are located along Port Joli Harbour, approximately 28 km southeast of Liverpool, Queens County, Nova Scotia. These pegmatites form a series of semi-parallel veins and dykes, which vary in thickness from about 5 cm to 1 m. Devono-Carboniferous monzogranites of the Port Mouton pluton are the main host rocks of these pegmatites.

Zonation of these dykes is chemical, mineralogical, and structural. The Wickwire pegmatites are different from most pegmatites in the region because they contain beryl and rarely have aplitic material in the core zones. The zonation results from the dual nature of the pegmatite; the border and wall zones are of an igneous origin, whereas the core is of a hydrothermal origin.

This thesis uses techniques such as petrographic microscopy, fluid inclusion analysis, X-ray fluorescence, X-ray diffraction and electron microprobe analysis to solve the problems of zonation of and origin of the Wickwire pegmatites.

Chapter 1: Introduction to Pegmatites

1.1 Introduction

In general, pegmatites are diverse rocks and exhibit highly variable mineralogy, morphology, texture, and geochemistry. Pegmatites are extremely coarse-grained rocks containing mainly K-feldspar, plagioclase, quartz, muscovite, and biotite, and they may contain accessory minerals such as beryl, garnet, and spodumene. Pegmatites typically form veins, dykes, or pods, and may show structural, mineralogical, and chemical zonation. The chemical composition of a pegmatite varies depending on the processes active during its petrogenesis, crystallization, and emplacement. Pegmatites are generally of igneous or metamorphic origin. This thesis presents the study of a granitic pegmatite located near Port Joli, Nova Scotia. The purpose of this thesis is to determine the composition, nature of the zonation, and the origin of that pegmatite based on qualitative and quantitative observations of the mineralogy and morphology of the pegmatite.

1.2.1 Physical Characteristics of Pegmatites

Pegmatites form many distinct morphological types including dykes and veins, schlieren, stockworks, and pods, e.g. bulbous masses, turnip-shaped bodies(Cerny,1982). The dimensions of pegmatites vary from several millimetres wide by 10s of cm long, e.g small veinlets in migmatites, to 300m wide by 2km long, e.g the Bikita pegmatite in Zimbabwe(Cerny,1982).

Generally, pegmatites are of two physical types, namely simple and complex. Simple pegmatites are unzoned, and are chemically, mineralogically, and texturally homogeneous(Guilbert & Park,1986).

This type of pegmatite forms cross-cutting veins of all shapes and sizes not structurally controlled by the host rock(Raguin,1965). Complex pegmatites are commonly zoned, and have chemical, textural, and mineralogical heterogeneities(Guilbert & Park,1986). Complex pegmatites are more massive than vein-like, and have shapes controlled mainly by the structure of the host rock, i.e. minerals arranged in parallel zones that conform to host rock boundaries(Raguin,1965).

Cameron et al.(1949) describe the internal structure of zoned pegmatites as follows:

1.Zones(1^{ary} feature) Border 5-20% of the pegmatite width
Wall 10-30% of the pegmatite width
Intermediate 0-30% of the pegmatite width
Core 30-50% of the pegmatite width

2.Replacement bodies- metasomatic origin,2^{ary} features(Jahns & Burnham, 1969)

3.Fracture fillings- igneous or metamorphic origin, 2^{ary} features.

A zone is a concentric shell or layer of primary crystallization only, whereas replacement bodies and fracture fillings cut the zonation (Guilbert & Park, 1986). Chemical and mineralogical zonation commonly overprint this structural zonation (Fig.1.2.1b). In general, the system of Cameron et al. is a classic, and is still used by the U.S.G.S..

1.2.2 Mineralogy and Texture of Granitic Pegmatites

In addition to feldspar, quartz, and mica, granitic pegmatites contain a variety of minerals as follows: a)alumino-, beryllo- and borosilicates, b)phosphates and c)oxides of U, Th, LREE, Ti, Nb, Ta (Cerny,1982). The following table presents the main and rare accessory minerals of pegmatites.

Table 1.2.2a

Main Accessories	Rare Accessories
garnet, schorl, beryl, lepidolite, amblygonite, apatite, cassiterite, spodumene, petalite, wolframite	hafnon, thorite, pollucite rhodozite, eucryptite, stibiotantalite elbaite, zinnwaldite

Pegmatites containing one or more accessory minerals are mineralized, whereas pegmatites lacking such minerals are barren. The proportions of phases commonly vary across zoned pegmatites and the rare accessories are generally in core zones (Cerny,1982)(Table 1.2.3a).

The system Albite-Orthoclase-Quartz-H_2O approximates the main mineralogy of granitic pegmatites (Jahns & Tuttle,1963)(Fig.1.2.3a). Normative plots in the system Ab-Or-Q-H_2O illustrate that granitic pegmatites have a dominantly eutectic composition (Fig.1.2.3b). This agrees with the high modal ratios of K-feldspar to albite and with the relatively constant modal percentage of quartz, at about 25%(Raguin, 1965). Water lowers the solvus of the system, but does not affect the composition of the minerals. Water accounts in part for the coarse-grained nature of and the abundance of hydrous phases (e.g. micas) in granitic pegmatites (Cerny,1982;Jahns & Burnham,1969;Raguin,1965).

Pegmatites are exceptionally coarse-grained rocks, but in zoned pegmatites, massive quartz is commonly found in the core. Raguin (1965) defines the grain sizes of pegmatites as follows: 1.fine-grained, <2.5cm, 2.medium-grained, 2.5-10cm, 3.coarse-grained, 10-30cm, and 4.very coarse-grained, >30cm. Pegmatites commonly have graphically intergrown phases and lack a fine-grained groundmass, but a matrix of massive quartz is common(Raguin,1965). Grain size as well as mineralogy can vary within a given pegmatite, and in general, zoned

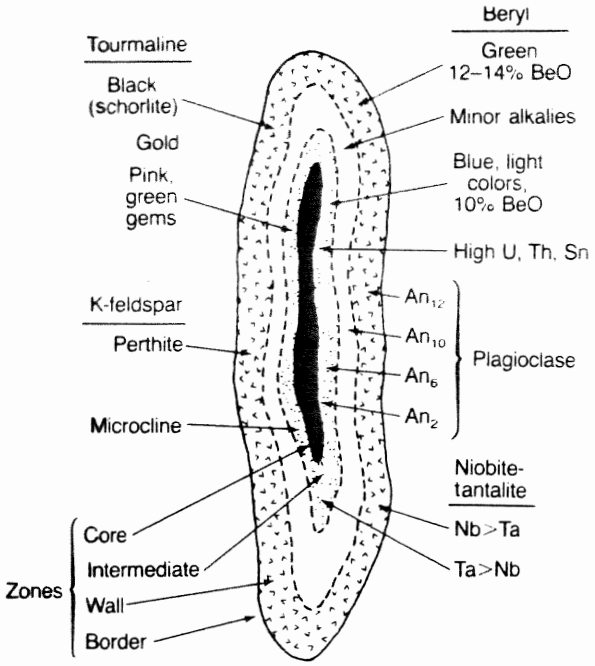

Fig.1.2.1a Guilbert & Park,1986

. Cryptic zoning from wall zone to core in individual pegmatite mineral spe
mposited from Cameron et al., 1949.)

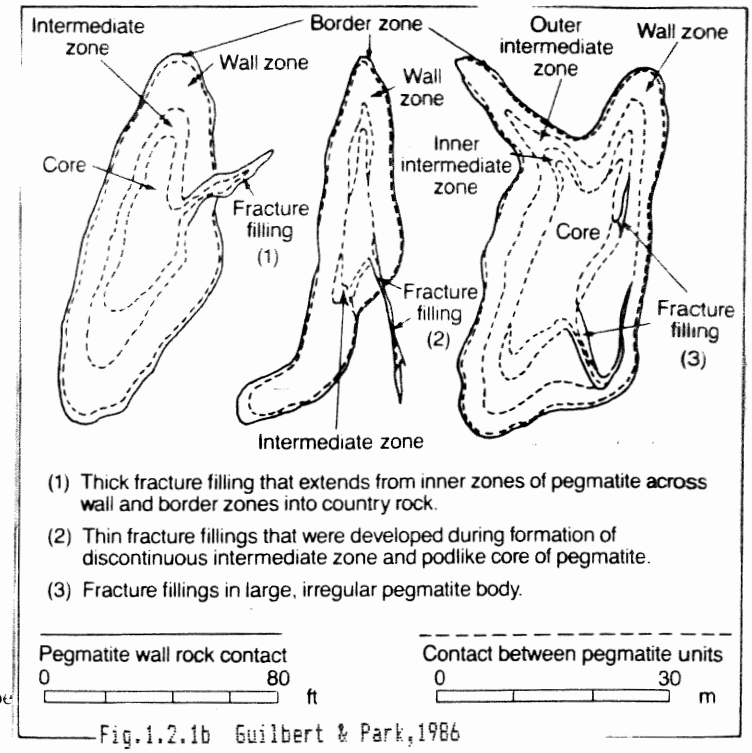

Fig.1.2.1b Guilbert & Park,1986

Č E R N Ý - ANATOMY AND CLASSIFICATION

Fig.1.3a Vlasov's classification scheme Cerny,1982

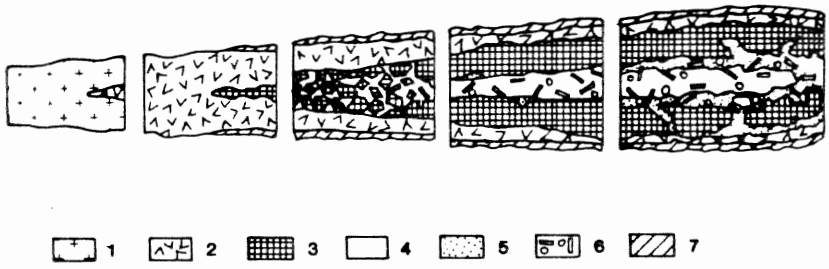

Fig. Schematic section of different textural-paragenetic pegmatite types of Vlasov (1952). 1 - pegmatite of granitic texture; 2 - graphic pegmatite; 3 - blocky K-feldspar, spodumene (oligoclase); 4 - blocky and core quartz; 5 - replacement zone (albitization with muscovite, beryl, tantalite, etc.); 6 - crystals of rare-element accessory minerals; 7 - muscovite + quartz + albite border fringe.

Table 1.2.3a Mineralogy of Pegmatite Zones
N.B. Most accessories listed in Table 1.2.2a occur in any zone, and are not listed here.
(after Guilbert & Park, 1986)

Plag + Qz + Musc	
Plag + Qz	Border Zone
Qz + Plag + Ksp + Musc + Bt	Wall Zone
Ksp + Qz	
Ksp + Qz + Plag + Amblygonite + Spodumene	
Plag + Qz + Spodumene	
Qz + Spodumene	Intermediate Zone
Micas + Plag + Qz	
Qz + Ksp	
Ksp + Plag + Micas + Qz	Core Zone
Qz	

pegmatites increase in grain size from the border to core zones, whereas unzoned pegmatites exhibit less variable grain sizes (Cerny, 1982;Guilbert & Park,1986).

1.2.3 Geochemistry of Granitic Pegmatites

In general, pegmatites have a granitic bulk composition, and therefore have major element contents similar to granites (Fig.1.2.3c). The most common deviations from an average granitic composition in pegmatites manifest as low CaO, K_2O/Na_2O, high Al_2O_3 and low K/Rb, K/Cs, Ba/Rb, Rb/Cs, Nb/Ta, Th/U ratios. The relative abundances of most elements in pegmatites, especially the trace elements, differ significantly from the abundances of the elements in the earth's crust; the only elements falling in the same order of relative abundance are O, Si, Al, and Nb (Fig.1.2.3d).

1.2.4 Geological and Geothermobarometric Environments of Pegmatites

Granitic pegmatites are present in all tectonomagmatic cycles throughout geologic time since the Kenoran (3.9-3.7 Ga). Pegmatites initially formed when sialic crustal fragments melted, and commonly occurred in variable grade metamorphic terranes and igneous bodies.

Pegmatites are stable over wide ranges of T-P space(Cerny,1982). Based on depth data from Ginsburg (Cerny,1982) and a modest geobarometric gradient of 1kb/3km, granitic pegmatites crystallize at depths and pressures ranging from 1.5km and 0.5kb to 11+km and 3.7+kb. Marmo (1971), Guilbert & Park (1986), and Cerny (1982) agree that the average temperature of formation of granitic pegmatites ranges over 200-700°C. Jahns & Burnham (1969) suggest that pegmatitic melts

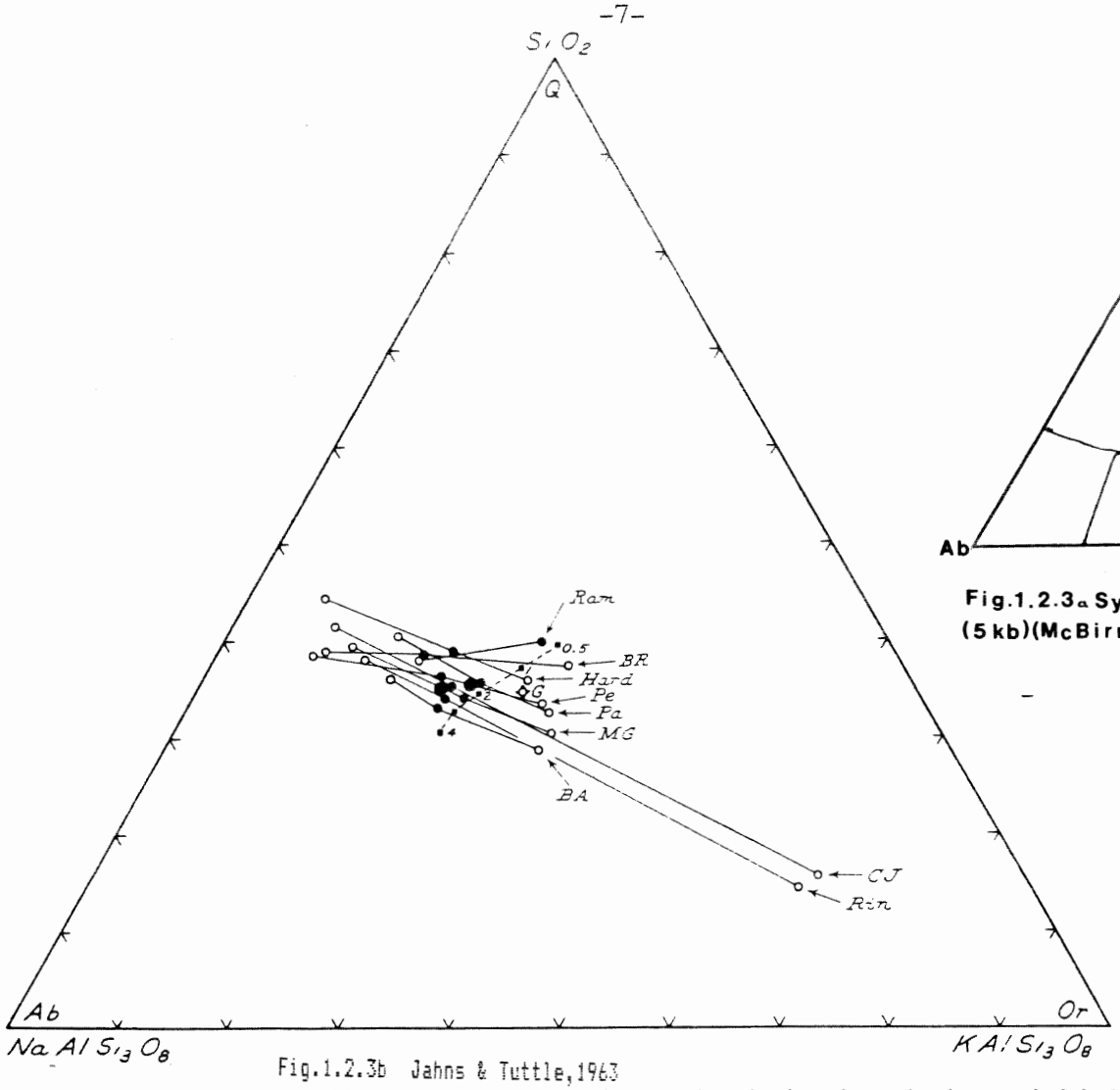

Fig.1.2.3b Jahns & Tuttle,1963

FIG. [illegible]. Distribution of normative albite, orthoclase, and quartz in pegmatite-aplite intrusives, related to trend of the isobaric minimum (dashed line) in the system $NaAlSi_3O_8$-$KAlSi_3O_8$-SiO_2-H_2O under water-vapor pressures ranging from 0.5 to 4 kilobars. G—normative plot for average of 571 analyzed granitic rocks (Tuttle and Bowen, 1958, pp. 75, 79). ~~Other points~~ as follows:

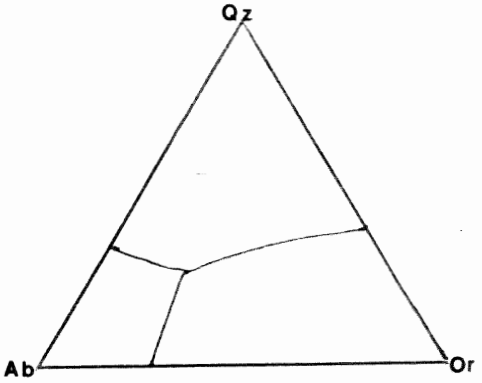

Fig.1.2.3a System Ab-Or-Qz (5 kb)(McBirney,1984)

Fig.1.2.3c Cerny,1982. CHEMICAL COMPOSITIONS OF GRANITIC PEGMATITES

	8	9	10	11	12
SiO_2	74.25	73.12	74.5	72.82	72.82
TiO_2	0.10	-	0.05	0.02	0.03
Al_2O_3	14.93	15.10	13.72	14.00	15.38
Fe_2O_3	0.56	0.93	0.50	0.14	0.45
FeO	0.40	0.29	1.39	1.00	1.15
MnO	-	-	0.02	0.06	0.07
MgO	0.67	0.58	0.17	0.30	0.31
CaO	1.81	1.19	0.46	0.40	0.70
Na_2O	3.21	3.43	3.77	2.30	3.51
K_2O	2.58	5.82	4.52	7.40	2.63
Li_2O	0.0035	0.0017	0.0017	0.10	0.47
P_2O_5	-	-	0.07	0.28	0.29
F	-	-	0.04	0.13	0.05
H_2O+	1.48	0.53	0.46	0.58	1.28
Total	100.18	100.42	99.67	99.53	99.14

Fig. 1.2.3c cont'd Granitoid Compositions (after McBirney,1984)

	Granodiorite	Granite	Leucogranite
SiO_2	69.45	71.35	75.34
TiO_2	0.36	0.32	0.18
Al_2O_3	14.88	14.32	12.87
Fe_2O_3	1.59	2.00	0.25
FeO	1.23	0.65	0.80
MnO	0.07	0.09	0.09
MgO	1.24	0.97	0.41
CaO	2.81	2.26	0.81
Na_2O	3.69	3.71	3.88
K_2O	3.29	3.13	4.38
F	0.05	0.06	0.03

Fig 1.2.3d Relative Order of Elemental Abundances in the Earth's Crust and Pegmatites

Crust	Pegmatite	Crust	Pegmatite
O	O	Sc	Hf
Si	Si	Nb	Nb
Al	Al	Ga	Ta
Fe	K	Li	Y
Ca	Na	Pb	U
Mg	Ca	B	Th
Na	Li	Th	Cl
K	Rb	Sn	C
Ti	Cs	Hf	Sc
P	Ba	Cs	Mo
Mn	Mg	U	W
F	Fe	Be	Bi
Ba	B	As	As
Sr	F	Ta	Sb
C	P	Ge	Zn
Zr	Sr	Mo, W	Cd
Cl	Mn	Tl	Cu
Rb	Be	Sb	Pb
Zn	Sn	Cd	Tl
Cu	Ti	Bi	Ga
Y	Zr		Ge

(after Cerny, 1982 and Smith, 1981)

/

Fig. 1.2.3d cont'd Trace Element Compositions of a Pegmatite and Granitoid (listed in ppm)

	Pegmatite	Granite		Pegmatite	Granite
La	14.14	-	U	9.92	-
Ce	36.87	13.04	Hf	3.31	4.79
Nd	30.53	7.11	Ta	9.73	0.98
Sm	4.71	1.81	Sc	0.65	-
Eu	1.12	0.75	Co	21.86	-
Tb	1.09	0.34	Y	46.97	-
Yb	9.24	1.49	Sr	33.10	598.0
Lu	1.26	0.21	Rb	314.63	19.00
Cs	0.86	-	Zr	10.89	2.48
Ba	151.14	-	Zn	9.60	110.0
Th	127.74	1.76			

(after Simmons et al.1987, and Douma, 1988)

separate and crystallize over a range of 1300-650°C. Such thermal variations are seen across the width of zoned pegmatites, where the core temeratures are typically lower than the border zone temperatures.

1.3 Definition and Classification Systems of Granitic Pegmatites

As defined here, the term 'granitic pegmatite ' refers to any extremely coarse-grained rock of igneous or hydrothermal origin having graphically intergrown crystals and commonly forming irregular dykes, lenses, or veins. Furthermore, granitic pegmatites contain mainly K-feldspar, plagioclase and quartz, and they may exhibit structural and/or mineralogical and/or chemical zonation patterns.

Morphology, structure, and mineralogy are suitable criteria for classifying pegmatites because these are the main features of any pegmatite. The first major distinction between types of pegmatites is simple versus complex, as discussed in Section 1.2.1 along with the classification of internal structures (Cameron et al.,1949). These two basic systems are mainly concerned with the morphological and structural aspects of pegmatites.

Another system accounting for both zonational and mineralogical variations in granitic pegmatites is that of Vlasov (1952)(Fig.1.3a). This system attributes textural and mineralogical variations to paragenesis.

Ginsburg et al. (1979) classify pegmatites depths of consolidation, mineralization, relation to igneous processes and metamorphic environment. In this system, there are 4 types of pegmatites, namely mariolitic, rare element, mica-bearing, and deep.

The metamorphic grade and depth of consolidation increase from the mariolitic to the deep pegmatitic environments, although mineralization is more common in the pegmatites of intermediate depth(Fig 1.3b).

A combination of these classification systems is used throughout this thesis, because several systems provide a better perspective on the nature of the pegmatite than one system.

1.4.1 Models for the Origin of Granitic Pegmatites

Several models explain the origin of granitic pegmatites and all assume that pegmatites are of igneous and/or metamorphic origin.

There are four basic igneous models for the origin of pegmatites, as follows: a)the injection or segregation of viscous magma, b)crystallization of a highly fluid magma (e.g. 8-10% free water), c)anatexis or palingenesis of granitoid parents, and d)crystallization of hot, silica-saturated aqueous solutions derived from granitic magmas (Cerny,1982;Guilbert & Park,1986). These models predict that granitic pegmatites evolve as late stage differentiates resulting from an intrusive event, whether or not they are truly magmatic phases.

Several observations support the igneous origin of granitic pegmatites. First, the graphic textures of quartz and feldspar, rather than predominantly poikiloblastic feldspars, suggests an igneous origin for graphic pegmatites (Guilbert & Park,1986). Secondly, most granitic pegmatites form close to granitoid intrusions, and commonly cut granitoids (Cerny,1982). Thirdly, zoned pegmatites commonly exhibit plagioclase-rich walls grading to K-feldspar-rich cores, suggesting that the paragenesis of pegmatites is governed by

Bowen's reaction series (Guilbert & Park,1986). Fourthly, rare element pegmatites commonly have trace element contents similar to nearby granitoids, suggesting that such pegmatites originate from igneous bodies. Lastly, fluid inclusion studies of some shallow pegmatites yield temperatures as high as 1200°C, well within the igneous regime (Jahns & Burnham,1969).

1.4.2. Metamorphic Models of the Origin of Granitic Pegmatites

The three basic metamorphic models of the origin of pegmatites are as follows: a)recrystallization of granitoids under metamorphic conditions(i.e. variable T & P, water-rich), b)anatexis of igneous or metamorphic rock at high temperatures in a metamorphic regime, and c)replacement or metamorphic differentiation (metasomatism)(Cerny, 1982).

Several observations support a metamorphic origin for granitic pegmatites. First, some granitic pegmatites occur in medium to high grade metamorphic terranes (e.g. migmatitic) lacking signs of obvious igneous activity (e.g. presence of granitoids). Secondly, the occurrence of identical metamorphic index minerals in both a metamorphic host and enclosed pegmatite is common in metamorphic terranes (Winkler,1967;Cerny,1982). Thirdly, the presence of highly poikiloblastic and/or pseudomorphic minerals may support the metamorphic origin of pegmatites, if not the metamorphic overprinting of pegmatites (Winkler,1967). Lastly, the presence of banded quartz commonly rich in large, isolated, euhedral, inclusion-rich, relatively high-temperature minerals such as almandine and beryl suggest a hydrothermal or metamorphic origin.

1.4.3 Models for the Generation of Zonation in Granitic Pegmatites

Several hypotheses explain the zonal variations of many pegmatites such as the arrangement of zones, apparent chemical gradients and the paragenetic consistency of zones among different pegmatites (Guilbert & Park,1986).

The zones result from fractional crystallization of a residual melt under disequilibrium conditions (i.e. continuous reaction between crytals and melt) (Guilbert & Park, 1986). In this case, the sequence of minerals from the border to the core of the pegmatite should correspond to Bowen's reaction series. A second hypothesis involves the precipitation of minerals along the walls of fractures from an aqueous solution of constantly changing composition (Guilbert & Park, 1986). A third hypothesis involves crystallization of a single injection of water-rich magma, differentiating into immiscible fluids upon ascent (Cerny,1982). Cerny(1982) also proposes that zonation develops as fractures in host rocks are filled by increasingly fractionated residual melts stratifying in reservoirs.

1.4.4 Conclusions

The following information is useful when examining any pegmatite:

1. Granitic pegmatites are commonly composed of quartz, feldspars and micas, and generally form very coarse-grained dykes in igneous and/or metamorphic terranes.

2. Granitic pegmatites may exhibit chemical(cryptic), mineralogical, or structural zonation, and may or may not be mineralized.

3. Classification of granitic pegmatites based on structure, mineralogy, chemistry, or field relations is useful, and many such

classification systems exist. Any one pegmatite may or may not fit into any or a combination of such systems.

4. Any given pegmatite may be of igneous and/or metamorphic origin, but the origin should not be pre-judged before the pegmatite is completely examined, regardless of the nature of the host rock.

1.5 Approach to Investigation

This thesis examines the field relations, petrology, and mineral chemistry of the pegmatite and host rocks at Port Joli, and uses the information in Chapter One to discern the nature and origin of the pegmatite. A fluid inclusion study of the main pegmatite and a study of the bulk rock compositions of the host rocks also help to place constraints on the origin of the pegmatite, e.g. depth of emplacement, temperature, nature of the protolith. The information in Chapter One serves only as a guide to pegmatites; the Port Joli pegmatite may or may not fit any, some, or all of the guidelines presented.

Fig. 1.3b Summary of Ginsburg Classification System of Granitic Pegmatites (after Cerny, 1982)

Type	Depth of Consolidation	Environment/Characteristics
Mariolitic	1.5-3.5 km	Low grade metamorphic/epizonal granites
Rare-element	3.5-7 km	Cordierite-amphibolite facies; differentiated allochthonous granite Li,Rb,Cs,Be,Ta mineralization
Mica-bearing	7-11 km	Almandine-amphibolite facies; anatectic from allochthonous granite REE, mica mineralization
Deep	>11 km	Granulite facies, associated with migmatites, rare mineralization, no obvious granitic parents.

Chapter 2

Field Work

Section 2.1 : Introduction

Sections 2.2 to 2.4.4B present the field relations, appearances, and mineralogies of a zoned pegmatite and its host rocks located at Port Joli Harbour, Nova Scotia. The procedures used during the study are as follows: 1. reconnaissance and area selection, 2. mapping of the selected area using plane tabling procedures, 3. collection of samples and drill core, and 4. sketching and photographing of pegmatites and host rock.

Section 2.2 : Geographic Setting

The Wickwire pegmatites, named after local residents Dr. and Mrs.J.C.Wickwire, are located approximately 28 km southeast of Liverpool, along Port Joli Harbour, Queens County, Nova Scotia. This area has NTS coordinates 20P 15D, and is located between 44 22.6' and 44 24.3' North Latitude and between 65 6.47', 65 7.58' West Longitude. The specific area mapped is about 5000 m^2 of coastal outcrop adjacent to Port Joli Harbour (See Map 1a). Access to this area is via Highway 103(~26 km southeast of Liverpool) and along the Port Joli Harbour road approximately 2 km southeast.

Section 2.3 : Regional Geology

The Goldenville Formation, composed mainly of greywacke, slate, and quartzite, is part of the Meguma Group. The Goldenville makes up the main regional lithology, and is of greenschist to amphibolite metamorphic grade in the Port Mouton region. This metamorphism

resulted from the Acadian orogeny (Keppie,1979). A contact metamorphic aureole overprints the regional metamorphic event and results from the intrusion of the Port Mouton pluton (Douma,1988). The Port Mouton pluton is a complex of Devono-Carboniferous tonalite-monzogranite of about 500 km^2 , and this pluton hosts the Wickwire pegmatites (Fig. 2.3a).

Section 2.4 : Description of Host Rocks of the Pegmatites

Three distinct, igneous rock types host the Wickwire pegmatites and they are designated as Units 1, 2, and 3, respectively. All pegmatites are designated as Unit 4, owing to the great number of veins/dykes. As defined here, a unit is a body of rock having a distinct mineralogy, modal percentage, and texture. Division of the outcrop into units is based on mineralogical and/or textural differences between different parts of the outcrop. Sections 2.4.1a through 2.4.4 present detailed descriptions of each unit.

Section 2.4.1a : Description of Unit 1

This unit contains mainly K-feldspar (~25%), quartz (~20%), plagioclase (~35%), accessory biotite, muscovite, and opaques, giving the unit a medium-grey to creamy-white appearance. On the basis of modal percentages, this unit is classified as a monzogranite (Fig.2.4.1a).

Two features define a foliation/fabric in the monzogranite as follows: a) common, flow-oriented laths of K-feldspar suspended in a relatively fine-grained groundmass and b) less common biotite stringers which are parallel to the orientation of the feldspar laths. This fabric remains relatively constant on the scale of the outcrop

Q = Quartz

A = Alkali feldspar

P = Plagioclase

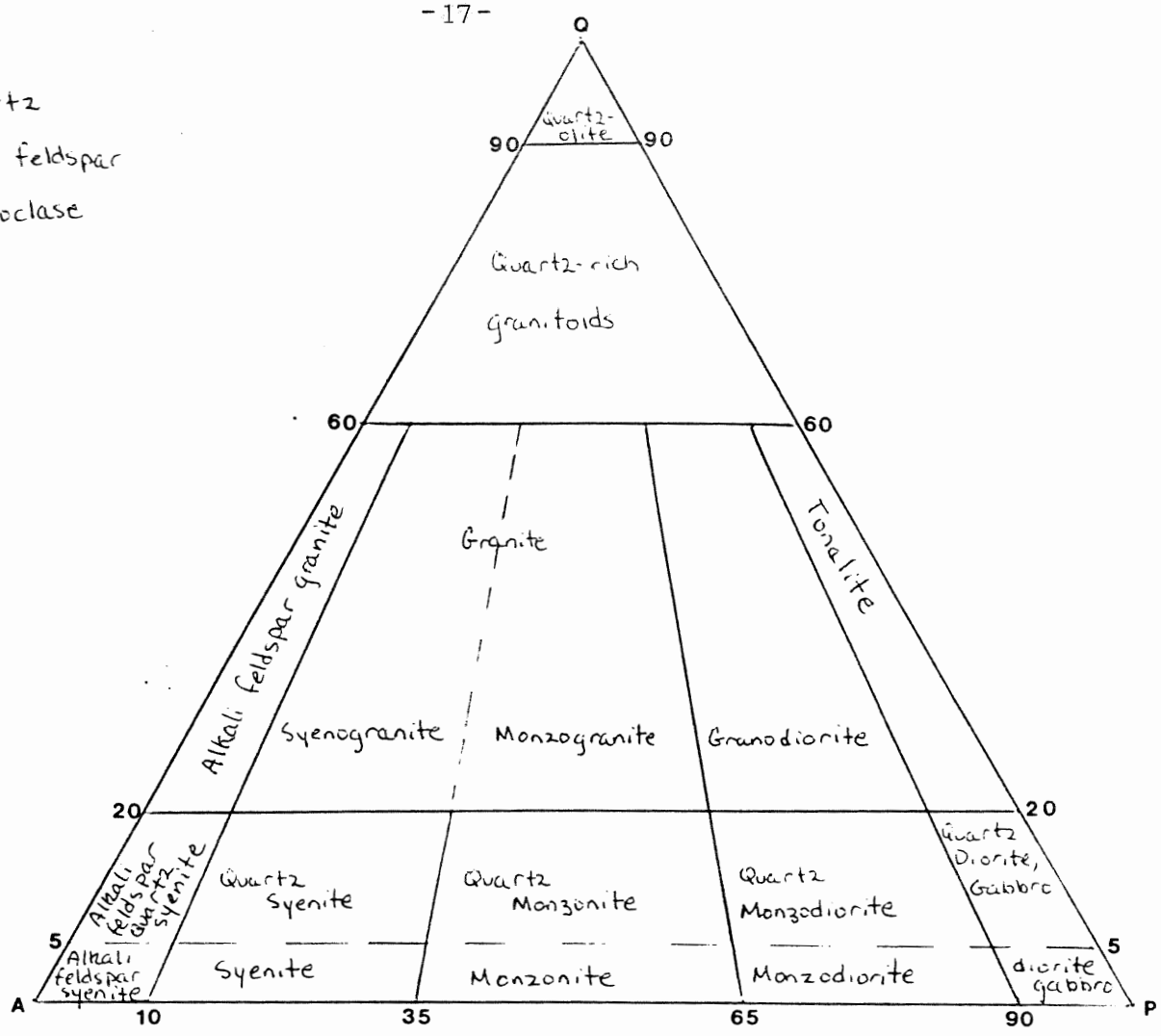

Fig. 2.4.1 a IUGS Classification for PLUTONIC ROCKS

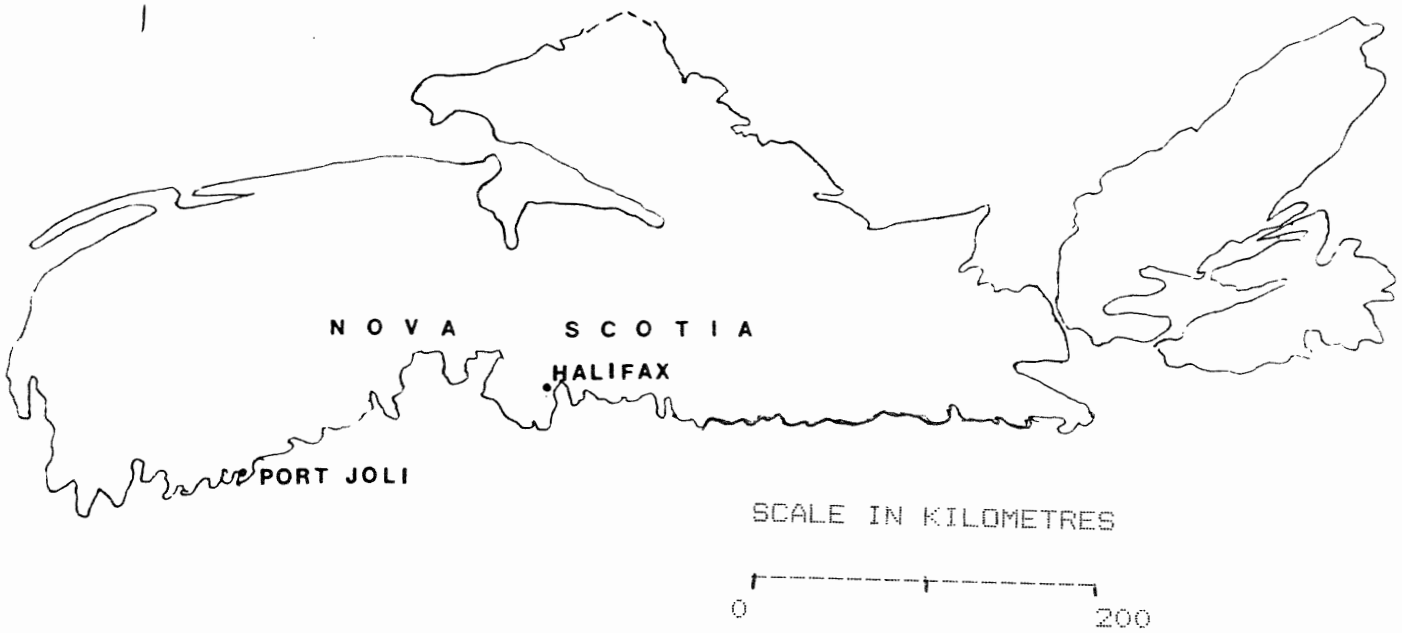

Fig. 2.3 LOCATION MAP

(Map 1a) (Photo 8).

Several pegmatite veins cut Unit 1, but the main pegmatite dyke, D4, does not cut Unit 1 (Map 1a). The pegmatite/Unit 1 contacts are distinct and sharp with little grain size variation in the monzogranite. The biotite content of the monzogranite, however, increases near the pegmatite contact.

Two small dykes of Unit 3 cut the monzogranite parallel to the foliation direction of the monzogranite, forming very diffuse contacts. Unit 2 also cuts the monzogranite, but it crosses perpendicular to the foliation in the monzogranite along the entire contact between the two units.

Randomly-oriented quartz and feldspar veins are common in Unit 1 and they are apparently not controlled by fracture sets in the monzogranite. Common felsic schlieren structures are prominent in the monzogranite at the western end of the outcrop, and they do not originate from any external intrusive unit.

Relatively mafic, aphryric, grey to black enclaves are common in Unit 1 and they are annealed and rounded rather than tectonically deformed (Photo 9). The contacts between Unit 1 and the enclaves are very sharp, and lack significant reaction rims. These enclaves are oriented with their long axes parallel to the flow foliation in Unit 1.

Thus, rock belonging to Unit 1 is monzogranitic, foliated, megacrystic, and relatively rich in mafic enclaves.

Section 2.4.2a : Description of Unit 2

Unit 2 comprises two subunits, namely 2a and 2b, or the main body

and banded aplite, respectively. This division is based purely on texture, as both subunits have a similar bulk mineralogy. These units contain K-feldspar (40%), plagioclase (~15%), quartz (~25%), and accessory biotite, muscovite, and garnet. Under the IUGS classification system, both units have a syenogranitic bulk composition, and are transitional to monzogranite. Unit 2 is called an aplite owing to its fine grain size and equigranular, saccharoidal texture. Unit 2 is light orange-yellow to white with local dark patches rich in biotite. The main aplite body has a homogeneous texture except for common pegmatitic inclusions.

The aplite is the second oldest phase because : a) the pegmatites cut the aplite, b)Unit 3 cuts the aplite and stopes blocks of aplite from the main unit, and c)the aplite cuts Unit 1. The banded aplites associated with the main pegmatite originate from Unit 2a, but are traceable only to one of the non-banded aplite bodies.

The main structural feature of these aplites is the banded appearance (Photo 11). These bands are multiple intrusions of aplite having an average width of 15 cm and biotite-rich contacts. In general, the contacts of Units 2a and 2b with the pegmatites and Unit 1 are sharp, exhibiting almost no grain size variation, whereas the Unit 2-Unit 3 contacts show smaller grain sizes and less biotite in Unit 3.

Also significant are the rectangular, stoped blocks(15 cm X 100 cm on average) of banded aplite in Unit 3. These blocks form sharp contacts with Unit 3, and several of them have tensional/torsional fractures filled by Unit 3 (Photo 10). These fractures result from the flowage of Unit 3 during intrusion, because they are commonly

perpendicular to the principal axes of the stoped blocks and to the foliation in unit 3, and parallel to the foliation in Unit 1.

In summary, Unit 2 is aplitic, syenogranitic, commonly banded, and rich in pegmatitic inclusions.

Section 2.4.3a : Description of Unit 3

Unit 3 contains quartz (~20%), K-feldspar (~15%), plagioclase (~50%), biotite (~15%), and muscovite (5%), giving it a flannel grey appearance. Unit 3 is a granodiorite, and is transitional to monzogranite.

The granodiorite is equigranular and medium-grained, lacking the megacrystic feldspars characteristic of Unit 1. Unit 3 contains rare, lensoid-shaped biotite inclusions and aligned biotite and feldspar crystals that define a foliation in the rock. This foliation results from flowage of the originally molten rock, and varies from parallel to the eastern contact with Unit 2a to semi-parallel to the contact with the main pegmatite. In general, Unit 3 is biotite-rich near contact zones.

Fewer pegmatite veins cut the granodiorite than cut Unit 1, but the main pegmatite contains small stoped fragments of the granodiorite. These fragments make up some of the darker fine-grained inclusions within the pegmatite. The granodiorite also contains large stoped blocks of aplite and irregularly-shaped pegmatitic inclusions.

The pegmatite-Unit 3, and Unit 3-Unit 2 contacts are generally sharp, with a slight decrease in grain size of Unit 3. Two small granodiorite dykes cut Unit 1 parallel to the foliation direction of

Unit 1 until they reach the former contact region between Units 1 and 2, where at least one dyke is semi-parallel to the former contact(i.e. normal to the foliation direction of Unit 1).

Several isolated masses ($1m^2$) of megacrystic, euhedral feldspars (~6 cm across) are found only in Unit 3 and are not traceable to any other units (Photo 7). Unit 3 also contains uncommon mafic enclaves similar in appearance to those in Unit 1.

In summary, Unit 3 is granodioritic, foliated, aphyric, poor in enclave content, and relatively rich in isolated masses of megacrystic feldspars.

Section 2.4.4a : Description of Main Pegmatite (D4)

Because the main pegmatite was the fourth dyke mapped, it is designated as **D4** (i.e. dyke #4)(Map 1a).

The main dyke contains mainly quartz (~45%),K-feldspar (~35%), plagioclase (~20%), muscovite (~15%), accessory garnet (~10%), rare biotite (<5%), and beryl (1-2%). Because the main dyke is zoned, these proportions vary across the zones, but are constant within a given zone (Fig.2.4.4). The average grain size in D4 is ~2-3 cm (medium-grained pegmatitic after Cameron et.al.,1949), and the colour varies from creamy-white near the walls to grey-blue in the quartz-rich core. The pegmatite has a dominantly syenogranitic composition, and is transitional to alkali feldspar granite (Fig. 2.4.1a).

Mineral descriptions, in order of modal abundance, are as follows:

Quartz: The quartz varies in texture from very fine-grained to massive and crystals are commonly anhedral. Most of the quartz is clear, and is banded in the core of the pegmatite, indicating relatively continuous precipitation from a hydrothermal fluid (Raguin,

1965).

K-feldspar & Plagioclase:Although there is about five times more K-feldspar than plagioclase in the pegmatite, both minerals have an average grain size of 1-6 cm, and both are commonly subhedral to euhedral, exhibiting common graphic intergrowths of quartz. The feldspars vary from white to pink-grey and the K-feldspars have common perthitic textures. Most of the crystals grow normal to the dyke walls and have more random orientations near the core of the pegmatite.

Muscovite: Muscovite commonly forms euhedral books having ~3 cm diameters and 2 cm widths. These books grow normal to contact zones with other units and normal to the strike of the pegmatite. The muscovite also contains rare, small, euhedral garnets.

Garnet: The garnets (almandine-spessartine-rich) are commonly euhedral and vary in size from 2 mm to 3 cm. Most of the smaller grains restricted to the feldspar-rich border zones, whereas the larger crystals grow in the core. The garnets do not grow near beryl-rich regions of the pegmatite.

Beryl: The rare beryl crystals are ~1 cm X 4 cm, commonly euhedral, and vary from a clear light green to mottled yellow-green. The crystals are typically fractured and have an unknown, frothy, white alteration on exposed terminae.

In general, the grain sizes of all minerals increase from the border to the core zone of the pegmatite.

Section 2.4.4b : Cross-Cutting Relationships & Structures

The main dyke cuts Units 2a and 3, but not Unit 1, although

pegmatites associated at least spatially and possibly genetically with D4 do cut Unit 1(Map 1a). The main dyke is parallel to the banding in Unit 2b, suggesting that the intrusion of the main dyke is fracture-controlled. The contacts with Units 2a and b are generally very sharp, with only a slightly finer grain size in the pegmatite, whereas the contact with Unit 3 varies over 3 cm, showing a greater reduction in grain size of the pegmatite and Unit 3. All units (i.e. 1, 2, & 3) contain isolated pods consisting of aplitic and/or pegmatitic material. These pods have an average size of 0.5 m and the contacts of these pods are distinct, varying over 0.5 cm.

The main structures in the pegmatite are the lensoid-shaped aplitic pods in the geometric core of D4 (Fig 2.4.4). These pods are ~3-20 cm wide, up to 1 m long, and are commonly asymmetrically distributed throughout D4 and they generally have diffuse contacts. These pods are of two types:1) a fine-grained (<1.5 mm), felsic aplite, and 2) a coarse-grained (2-3 mm), dark, biotite-rich aplite.

The first type of pod is homogeneous, contains mainly K-feldspar, plagioclase, quartz, and muscovite, and lacks any fabric. These pods are also aphyric, but are rich in biotite near the contacts. In general, these pods are weathered, exhibiting pits where feldspars must have been.

The second type of pod is grey to brown, and consists of mainly K-feldspar, quartz, and muscovite, with locally high concentrations of biotite. The darker pods are less homogeneous in texture, with a grain size range of 1-4 mm, and unlike the felsic pods, they contain rare garnets. Some of these mafic pods grade laterally into felsic pods.

Fig. 2.4.4a Modal Variations Across the Pegmatite

Mineral Zone	Qz	Ksp	Plag	Gnt	Musc	Beryl
Border	25%	60%	5-10%	2%	5-10%	-
Wall	35%	40%	10-15%	-	10-15%	-
Core	65%	20%	< 5%	5%	5%	1-3%

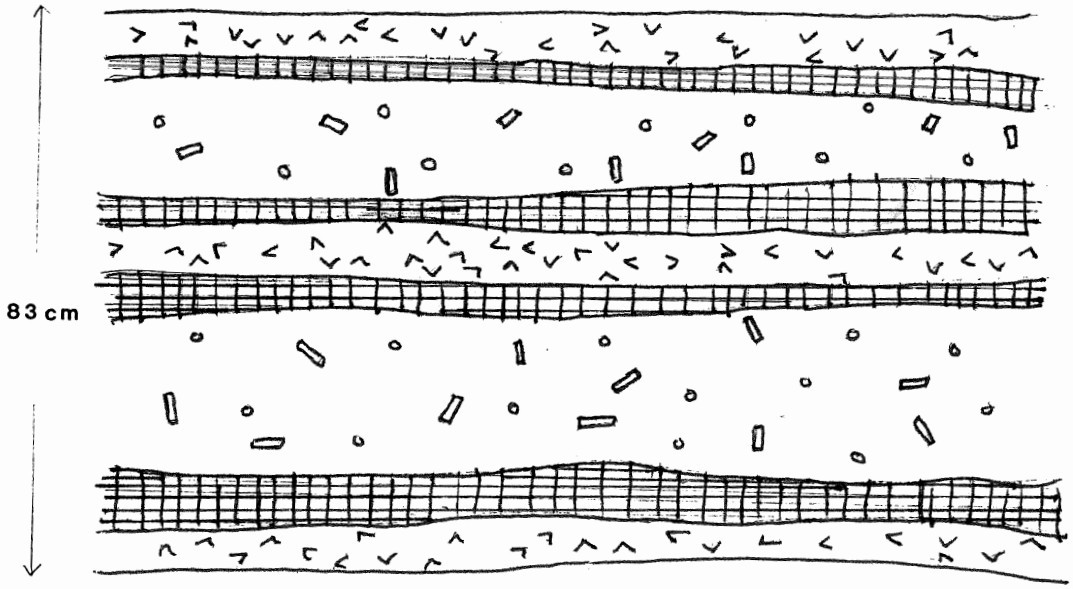

Fig. 2.4.4b Schematic of Pegmatite Zonation

Border zone- graphic pegmatite
Vlasov's Section 2

Wall zone- blocky K-feldspar
Vlasov's Section 3

Core zone- banded quartz + accessories
Vlasov's Section 7
(after Cerny,1982;see Fig 1.3)

The other main stuctural feature of D4 is the textural and mineralogical zonation, described below.

Border Zone: The border zone is 0.5-2.5 cm wide and consists mainly of graphically intergrown feldspars, small amounts of quartz, rare, euhedral garnets(1-4 mm across), and uncommon muscovite books(0.5 mm across). The feldspars have an average size of 0.5-0.8 mm and generally grow normal to contacts.

Wall Zone: This zone is 3-4 cm wide and consists of mainly K-feldspar and plagioclase, with grain sizes of 1-3 cm. The feldspars are more perthitic and the muscovite books larger and thicker than in the border zone. Both the feldspars and mica books are only sub-normal to the border zone. Garnet (almandine-spessartine-rich) is common, and varies in size from 1 mm-1.5 cm. The garnets have common quartz inclusions unlike the garnets of the border zone.

Core Zone: The core averages 10-15 cm across, and contains up to 70% quartz, more than any other zone. The quartz is generally massive, containing mainly euhedral K-feldspars up to 4-6 cm across. The quartz is very clear and banded near the wall-core contact. The garnets are less common but larger than in the other zones. Beryl crystals are present in the core (crystals described in Section 2.4.4a).

A sketch and photographs, below, summarize the textural and mineralogical variations across the main pegmatite (photographs 1-6).

2.5 Conclusions

From the evidence presented in this chapter, several conclusions are evident:

1. The main pegmatite is both structurally and mineralogically zoned.

2. Unit 1 is the oldest, followed by Units 2, 3, and 4.

3. Units 1 and 3 are very similar mineralogically and texturally, except for mineral proportions.

4. Because the main pegmatite parallels the banding in Unit 2, it is probable that the intrusion of the pegmatite is fracture controlled.

5. The aplitic pods in the core of D4 may be replacement bodies or late fracture fillings.

6. The intimate association between the pegmatite and the banded aplite suggests that the pegmatite originated as a late stage, fluid-rich differentiate of the aplite.

1
3

2

1. Fine-grained felsic aplitic pod in core of pegmatite. Note surrounding coarser material (lens cap for scale).

2. Aplite-pegmatite contact. Note increase in grain size away from contact in the pegmatite. Dark patches are muscovites growing normal to the contact. Garnet near bottom of photo(brown colour).

3. Zonation of pegmatite; contact with granodiorite. Note quartz-rich core and feldspar-rich wall and contact zones. Corresponding schematic in Fig. 2.4.4b at widest point of pegmatite. Note highly graphic nature of the pegmatite.

4

5

6

4. Border zone-large garnet in center of photo; local quartz-rich patches. Dark patches are muscovite-note increasing muscovite content from contact (right) to wall zone(left).

5. Perthite and K-feldspars including garnets. Note that the larger feldspar at the bottom of the photo floats in a quartz matrix. Garnets grow mainly in the feldspars.

6. Large aplitic pod; grades from felsic(top) to mafic(bottom). Note coarser material around the pod.

7

8

9

7. Isolated, megacrystic feldspars, and xenoliths in granodiorite. Feldspars are about 8 cm across. Note similar orientations of xenoliths.

8. Foliation in monzogranite defined by aligned feldspar laths. Foliation extends from left to right in photo. Quartz veinlet in upper left-hand corner.

9. Large xenoliths in the monzogranite. Xenoliths contain small felsic stringers not continuous with the monzogranite. Note that the xenoliths appear as fragments of a larger block.

10

11

10.Stoped, fractured aplite in granodiorite (1" drill hole for scale). Note the fractures normal to the long axis of the block. 11.Banding and pegmatite veins in banded aplite. Note the parallel nature of the bands. 12.Outcrop overview (main pegmatite diagonally across photo). Banded aplite and monzogranite to left of pegmatite, granodiorite to the right.

12

Chapter 3

Petrography

3.1 Introduction

Sections 3.2 to 3.5 present detailed petrographic descriptions of the four rock units described in Chapter Two. The descriptions are composites made from an average of 4 to 15 thin sections per rock type. The thin section samples are as fresh as possible, and come from the central and contact regions of the rock units.

3.2.1 Unit 1 : Overall Description

Average modal compositions of the monzogranite, based on 400 points for each of five slides, are: 36% K-feldspar (microcline + anorthoclase), 24% plagioclase(An_{05}-An_{42}), 23% quartz, 12% biotite, 4% muscovite and ~1% opaque minerals. The minerals are inequigranular and have an average grain size of 1.5-2 mm. The feldspars are 1.5-2 times larger than the other grains, forming a hiatal porphyritic texture.

The monzogranite shows only slight weathering, although most of the minerals are fractured. Most samples show a moderate foliation defined by aligned, subhedral feldspar laths.

3.2.2 Mineral Descriptions of Unit 1

a.<u>K-Feldspar</u>: The K-feldspar is mostly microcline and anorthoclase averaging 0.5-1.5 mm in size, and showing common, lensoid plagioclase exsolution lamellae. The anorthoclase and microcline contain small quartz blebs and are slightly weathered to sericite. Quartz grains form myrmekitic and cuspate structures with the K-feldspar.

b. <u>Plagioclase</u>: The plagioclase varies from albite to andesine, with

an average size of 1-3 mm. These crystals are commonly subhedral and twinned or concentrically zoned, and the lamellae of the twinned crystals are commonly bent. Semi-oriented quartz and apatite inclusions form a sieve texture along growth zones in the plagioclase. Biotite rarely overgrows the plagioclase.

c. Quartz: The quartz is anhedral, averages 1-2.5 mm across, and shows undulose extinction owing to the misorientation of subgrains by an average of 6°. The subgrains have grain shape and slight lattice-preferred orientations, showing the strain in the quartz. The quartz has common healed fractures and a few muscovite inclusions. The larger grains exhibit narrow mantle structures of relatively strain-free quartz.

d. Biotite: The biotite is red-brown to greenish-brown, reflecting the variable Fe content. These crystals have an average size of 0.2-2 mm and commonly form decussate aggregates. The biotite is commonly anhedral, although rare euhedral crystals overgrow the K-feldspar and plagioclase.

e. Muscovite: The muscovite is anhedral and varies in size from 0.5-2 mm. The crystals commonly form undeformed, decussate aggregates overgrowing some of the biotite crystals, suggesting that the muscovite grew after the quartz was deformed and after the biotite crystallized.

3.3.1 Unit 2 : Overall Description

The aplite has an average grain size of 2-3 mm, and has an average modal composition as follows: 42% K-feldspar (microcline, adularia), 26% quartz, 14% plagioclase (oligoclase, andesine), 8% muscovite, 4% biotite, 3% garnet (almandine-spessartine-rich), and ~1% opaques. Most grains are subhedral and equigranular, with the exception of common K-feldspar

phenocrysts.

3.3.2 Mineral Descriptions of Unit 2

a.K-feldspar: The K-feldspars have an average grain size of 1-3 mm and are commonly subhedral. The microcline exhibits cross-hatch twinning and parallel, lensoid lamallae, and includes rounded quartz and randomly-oriented biotite. There are common myrmekitic and graphic intergrowths with quartz at crystal boundaries and interiors, respectively. These crystals show undulose extinction, indicating a moderate degree of stress.

b.Quartz: The quartz has an average size of 1-2.5 mm, is anhedral, and forms aggregates. Fractures, undulose extinction, core and mantle structures, and lattice-preferred orientations of subgrains are common features. The quartz includes rare, blebby plagioclase and subhedral muscovite.

c.Plagioclase: The plagioclase averages 1-4 mm in diameter, and is commonly concentrically zoned with altered, Ca-rich cores. The main alteration, saussurite, is most common in the cores, and the degree of alteration increases with An content. The plagioclases include randomly-oriented apatite needles, muscovite, and blebby quartz.

d.Muscovite: The muscovite of Unit 2 is subhedral, averages 1x2.5 mm, and commonly forms decussate aggregates. The muscovite is rarely kink-banded, has slightly undulose extinction, and includes common apatite, rounded quartz and feldspar.

e.Biotite: The biotites average 1-2 mm across, are anhedral to subhedral and are dark reddish-brown, or more rarely, green. The aligned biotite defines a moderate foliation in the aplite. Zircon, quartz,

apatite and feldspar inclusions are common.

f.Garnet: The garnets are subhedral to euhedral, are pinkish-red to brown, and vary in size from 0.2-0.7 mm. Thin rims of opaque minerals and/or red Fe oxides partially border the garnets. These garnets are rarely fractured and are generally inclusion-free.

3.4.1 Unit 3 : Overall Description

The granodiorite has an average grain size of 0.5-1.5 mm,is slightly finer-grained and has a higher biotite and plagioclase content than the monzogranite. The modal composition of Unit 3 is as follows: 49% plagioclase (andesine), 18% quartz, 16% biotite, 13% K-feldspar, and 4% muscovite. The samples are equigranular and graphic, with rare microcline phenocrysts. The samples show little alteration, although the microcline exhibits albitization.

3.4.2 Unit 3 Mineral Descriptions

a.Plagioclase: The plagioclase is concentrically zoned, with Ca-rich cores exhibiting alteration to white mica. The zoned crystals are subhedral and highly fractured, and have common muscovite and quartz inclusions near the rims. Graphic intergrowth with quartz is also typical.

b.Quartz: The quartz grains are 2-3 mm across, are anhedral, and have slightly undulose extinction. The subgrains are highly misoriented(~11°) and exhibit a weak grain shape-preferred orientation. The amount of deformation decreases away from the pegmatite. There are few inclusions in the quartz and rare mantle structures are present.

c.Biotite: The biotite defines a weak foliation in the granodiorite, is commonly red-brown to green and averages 0.5 mm across. Pleochroic haloes and Fe oxide alteration are common, and the grains are relatively

inlusion-free. Rare, secondary, euhedral crystals are seen in the cores of plagioclases.

d.K-feldspar: The K-feldspar is anhedral, inclusion-free and ~1.5 mm in diameter. Most of the K-feldspar is microcline, which exhibits exsolution lamellae, symplectic intergrowth with quartz, and abundant fractures. In general, these feldspars are less altered than those of Unit 1.

e.Muscovite: The muscovite has an average size of 0.5 mm and forms decussate aggregates. Generally, the muscovite is not kinked or aligned, and is undeformed. Rare, rounded quartz and feldspar inclusions are also present.

3.5.1 Unit 4 : Border and Wall Zone Mineral Descriptions(Main Pegmatite)

The upper and lower 10 cm of the pegmatite are similar in texture to the granodiorite, except that the mineral proportions and grain sizes differ. The border and wall zones have a modal composition as follows: 35-70% K-feldspar, 0-25% plagioclase ($An_{>}$), 25-35% quartz, 5-10% muscovite, and 1-3% garnet (almandine-spessartine-rich).

a.K-feldspar: The K-feldspars average 3-7 mm across, are commonly subhedral and exhibit heavy alteration to white micas along cleavage traces. Common, lensoid exsolution lamellae and rounded quartz and feldspar inclusions are present, although the lamellae are generally bent owing to small shear zones. Graphic intergrowth with quartz is also common.

b.Quartz: The quartz averages 5 mm in diameter and has subgrains with average misorientations of 4-9°. The larger, strain-free grains have thin mantle structures.

c.Plagioclase: The plagioclase grains average 3 mm across, are

commonly concentrically zoned or twinned, and show alteration to sericite. The plagioclase includes microcline, quartz, and randomly-oriented apatite needles. Also, the zoned crystals exhibit common seive textures.

d.Muscovite: The muscovite averages 2 mm in length, and increases in size away from contacts. The grains form decussate aggregates and are commonly inclusion-free. Kinking and shearing of the crystals result from localized shear zones.

e.Garnet: The garnets are euhedral, up to 4 mm across, and are almost inclusion-free. These crystals contact all other phases in the border zone, but grow mostly in the plagioclases. The garnets commonly alter to epidote along numerous fractures.

3.5.2 Unit 4 : Core Zone Mineral Descriptions

The main minerals in the core region are quartz, K-feldspar, garnet, muscovite and beryl. Plagioclase is not present in significant quantity. Because the grains average more than 5 cm across, a good estimate of mineral percentages is impossible. An crude estimate is as follows: 65% quartz, 20% microcline, 5% garnet, 5% muscovite, 1% beryl.

a.Quartz: The quartz shows lattice- and grain-shape-preferred orientations, undulose extinction, and extensive fracturing. Parallel bands of alternating fine- and coarse-grained quartz spaced about 5 mm apart are common. This banded quartz is considerably more inclusion-rich than the quartz in any other rock type.

b.Microcline: The microcline is cross-hatch twinned and has linear inclusion trails of quartz and plagioclase. Alteration to white mica along the cleavage traces is common. The microcline also exhibits myrmekitic intergrowth with quartz along the crystal boundaries.

c.Garnet: The garnet is red-brown, euhedral and highly poikilitic, with 60-70% of the crystal volume composed of subangular quartz inclusions. Moderate alteration to Fe oxides along the rims and to saussurite along fractures is common. The garnet also includes muscovite and microcline along the rims.

d.Muscovite: The muscovite is euhedral, has a decussate appearance, and is slightly kinked. Quartz and randomly-oriented apatite needles are common inclusions in the muscovite.

e.Beryl: The beryl is always euhedral, light green in colour, and highly fractured. Rare fringes of frothy-looking alteration line some of the fractures. The beryl includes rare quartz and feldspar, and fluid inclusions are very abundant and visible at low magnification. Rare, weakly-oriented apatite needles are also common inclusions.

Figure 3.1 summarizes the modal estimates of all rock units.

3.5.3 Conclusions

Several conclusions are evident from the observations in this chapter:

1. The monzogranites and granodiorites are texturally and mineralogically similar, except that the granodiorites have a higher plagioclase content and are finer-grained.

2. The quartz from all rock types shows some degree of deformation. Because this deformation is not extensive and decreases away from the wall zone, the deformation may result from the intrusion of the pegmatite.

3. The wall and border zones of the pegmatite have a magmatic origin, whereas the core has a hydrothermal origin. The evidence for this is as

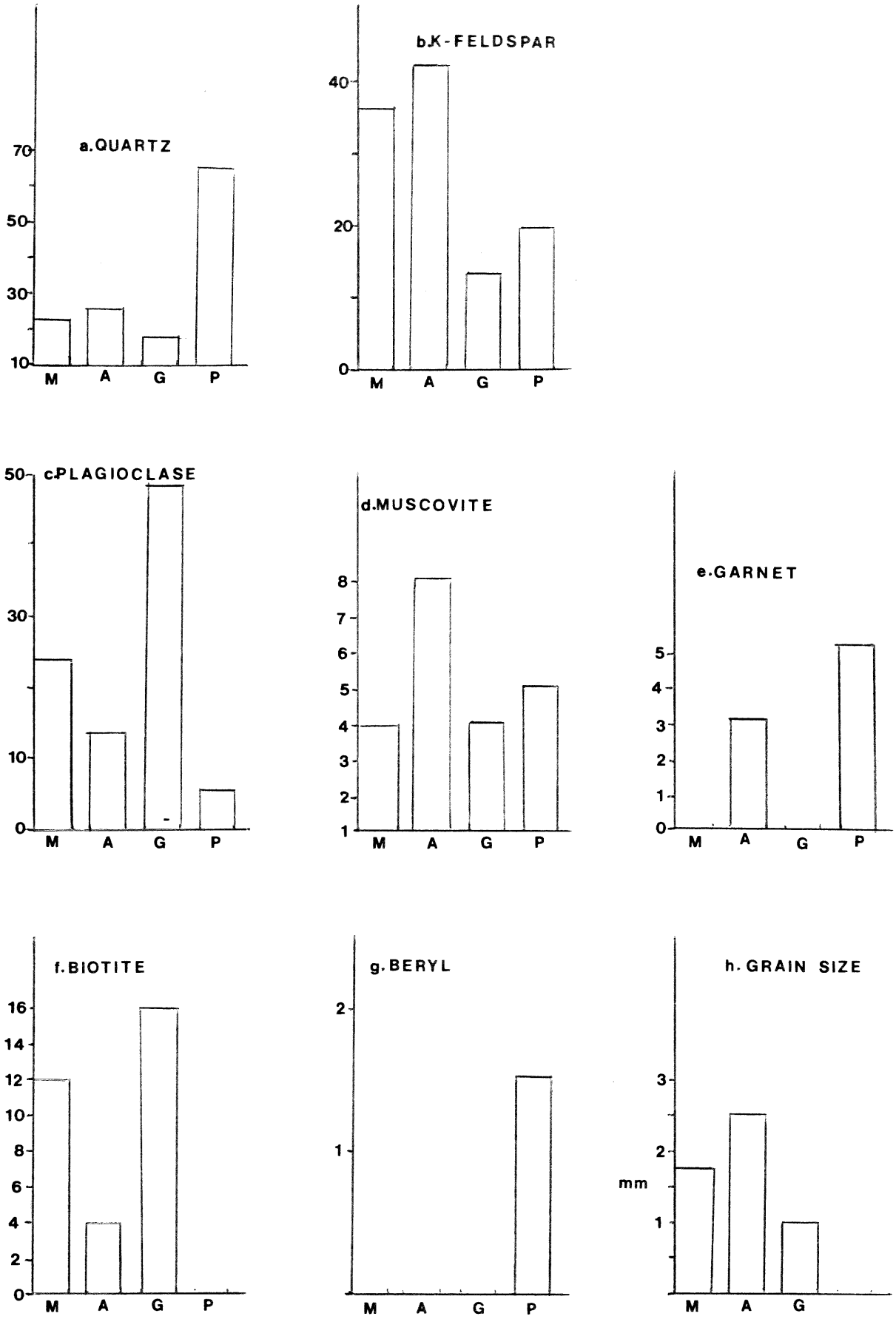

Fig. 3.1 Modal variations and grain size variations for all units. M=monzogranite(Unit 1), A=aplite(Unit 2), G=granodiorite (Unit 3), P=main pegmatite.

follows:

a.There are vast textural differences between the garnets at the walls and in the core of the pegmatite.

b.The minerals in the core zone are suspended and isolated in a matrix of massive, banded quartz (i.e. ~80% quartz in some regions, a proportion atypical of a granitoid system).

c.The quartz in the core of the pegmatite is banded much like agate, whereas the quartz at the wall and border zones is not banded.

d.The bulk composition of the core, as indicated by the modal proportions, is clearly not magmatic.

4. Some of the muscovite in Units 1, 2, and 3 is totally undeformed, suggesting that it grew after or during the episode of deformation, perhaps via fluid overprinting by the pegmatite.

5. The quartz in the core of the pegmatite is much less deformed than in other units, suggesting that the deformation of the other units and other parts of the pegmatite results from the intrusion of the pegmatite.

6. According to the mineralogical classification system of pegmatites by Varlamoff(1960), the Wickwire pegmatite is a Type 5 pegmatite, i.e. it contains muscovite, quartz, microcline, a few small beryls, and a small amount of albite. This also agrees with the classification of other pegmatites in the Port Mouton area by Kent (1959).

7. Some process operated to enrich beryllium in the core of the pegmatite, and another or the same type of process enriched Fe and Mn in the wall and core zones of the pegmatite (i.e. because no garnet is present in the border zone).

Chapter 4

Fluid Inclusion Work

4.1 Introduction

If the core of the pegmatite is hydrothermal in origin, as proposed in Chapter 3, then fluid inclusions in the core zone should have low homogenization temperatures and possibly high salinities (Roedder,1984). Examining the fluid inclusions in several garnets from the core zone should confirm whether the garnets and core zone are hydrothermal in origin, and reveal data about the composition of the pegmatitic fluid.

4.1.1 Background

As a crystal grows in a fluid-rich medium, pockets of fluid adhere to the crystal and become trapped. From this fluid, vapour exsolves and/or solid phases precipitate as the crystal cools. Upon reheating, the vapour and liquid phases in a fluid inclusion homogenize at a given temperature, T_h. The T_h provides an <u>estimate</u> of the temperature of crystallization for a given phase, but is prone to pressure effects. The freezing temperature of the fluid also reveals useful information.

The salinity of the fluid depresses its freezing/melting temperature. The amount by which the freezing point of the fluid decreases relative to H_2O is a function of the salinity of the fluid. Thus, by determining the freezing point of the fluid, the salinity is calculable. The salinity gives a fair estimate of the composition of the fluid phase present during precipitation/crystallization of the mineral phase in

question.

4.2 Description of a Typical Fluid Inclusion Pattern in Garnet

Figure 4.2a shows a sketch of the garnet described below. This garnet is about 80-90 microns thick and is extremely clear. The subsections below are descriptions of the garnet divided by focal depth into the crystal.

a.Uppermost 10 microns: The inclusions in this zone are highly variable in shape, size, and liquid to vapour ratio. They vary from rounded to semi-convoluted, and the vapour bubble is commonly located in the middle of the inclusion. These inclusions lie in a plane, and are randomly oriented within this plane. Inclusions in this focal range may be primary (i.e. formed during the growth of the crystal), because they define a plane parallel to a growth face of the crystal.

b.30-50 microns: The long axes of the inclusions in this range are parallel and oriented at a constant angle to a growth face of the crystal, and are, therefore, probably primary inclusions. These inclusions are commonly thin, necked, and cylindrical, and have liquid to vapour ratios of about 10:1. The vapour bubbles are generally at one end of an inclusion. Some of the larger inclusions are negative crystal forms, containing about 20% CO_2, and about 70% H_2O by volume. The larger inclusions contain visible, but unidentifiable, daughter minerals and single-phase vapour bubbles.

c.50-70 microns: These inclusions are commonly necked or rounded, and they line up very well in long strings, typical of secondary inclusions (Roedder,1984). The rounded inclusions commonly have one bubble occupying up to 25-30% of the volume of the inclusion. Daughter

minerals are generally absent from these inclusions. These inclusions are secondary or pseudosecondary in nature(i.e. formed after the growth of the crystal along fractures), because they lie in a plane not parallel to a growth face.

d.Lowermost 10 microns: The inclusions in this range are generally very large and irregularly shaped. The vapour bubbles are very hard to identify and some of these inclusions contain visible daughter minerals. These inclusions are probably primary in origin, because they do not define fractures, they are generally isolated, and some contain daughter minerals.

4.3 Freezing and Homogenization Temperature Data

Garnet is the mineral of choice for examination, mainly because any secondary inclusions must define fractures rather than cleavages (i.e. because garnet has no cleavage).

Most primary inclusions in the garnet freeze at -3.8°C, indicating salinities of about 6% (Table 4.3)(Fig.4.1b). The variation in freezing temperature suggests that a salinity gradient exists from the outer to inner core region. Such low salinities indicate that minerals such as KCl, $CaSO_4$, and silicates are probably present. Based on a CO_2 volume fraction of 20-25% in each primary inclusion , the pressure of homogenization for the liquid and vapour is 1.6-1.7 kb (Fig. 4.5) (Roedder,1984).

Most of the primary liquid + vapour inclusions homogenize at an average of about 220°C (Table 4.3)(Fig.4.1a). The presence of 1-, 2-, and 3-phase inclusions suggests that resurgent boiling occurred in the system. The bimodality of the T_h histogram suggests that an abrupt

Table 4.3a Freezing and Homogenization Data(Primary Inclusions)

Trial	T_h (C)	T_f (C)	$\%CO_2$	Salinity(%)
1	214.2	-3.8	15	6.4
2	214.3	-3.9	20	6.4
3	225.2	-3.7	20	6.39
4	225.4	-3.7	20	6.39
5	243.2	-3.6	25	5.99
6	243.0	-3.6	25	5.99
7	243.3	-3.8	20	6.4
8	235.9	-3.9	20	6.41
9	235.8	-3.9	20	6.41
10	236.0	-3.8	25	6.4
11	233.7	-3.6	10	5.99
12	233.5	-3.5	15	5.9
13	233.5	-3.5	15	5.9
14	215.6	-3.9	20	6.41
15	215.7	-3.8	20	6.4
16	212.9	-3.7	20	6.39
17	213.1	-3.7	20	6.39
18	203.5	-3.5	20	5.72
19	203.5	-3.5	20	5.72
20	203.5	-3.6	20	5.99
21	213.8	-3.9	25	6.41
22	214.0	-3.9	25	6.41
23	213.9	-3.8	25	6.4
24	216.2	-3.8	25	6.4
25	216.3	-3.9	25	6.41

Fig. 4.2a Garnet Sketch

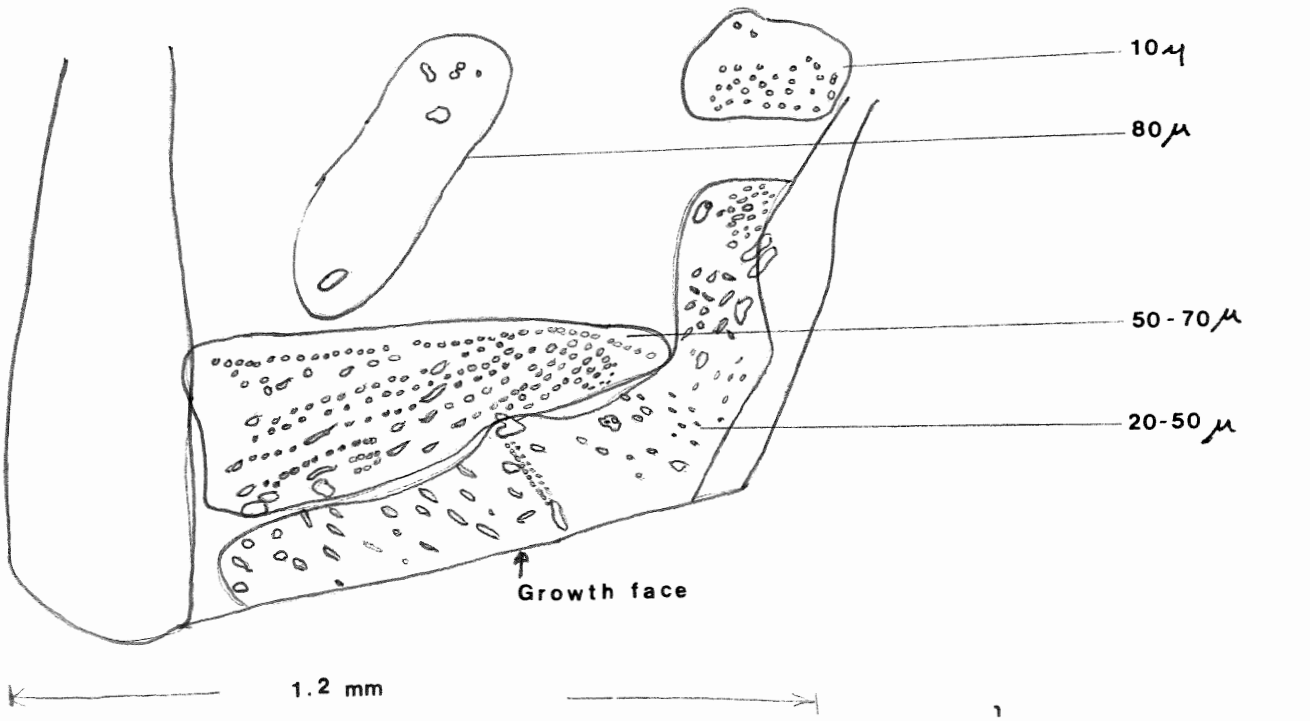

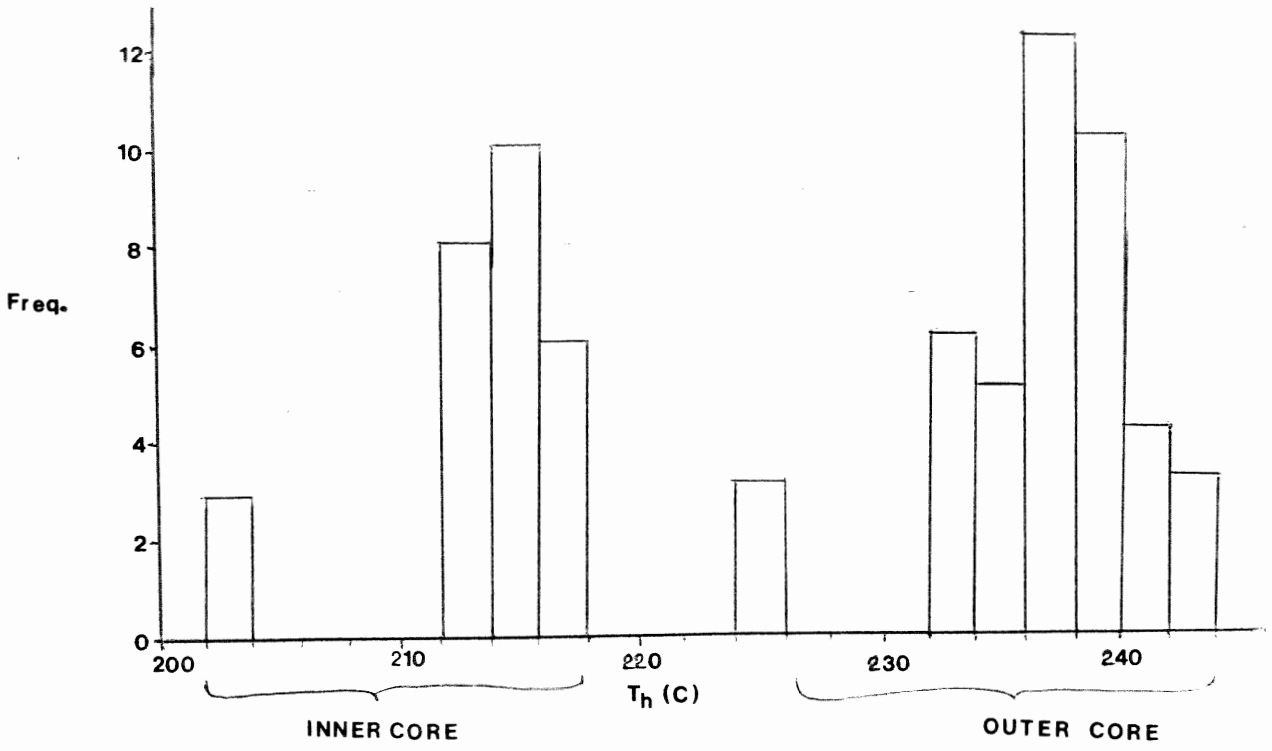

Fig.4.1a Freezing temperature histogram.

Fig.4.1b Homogenization temperature histogram.

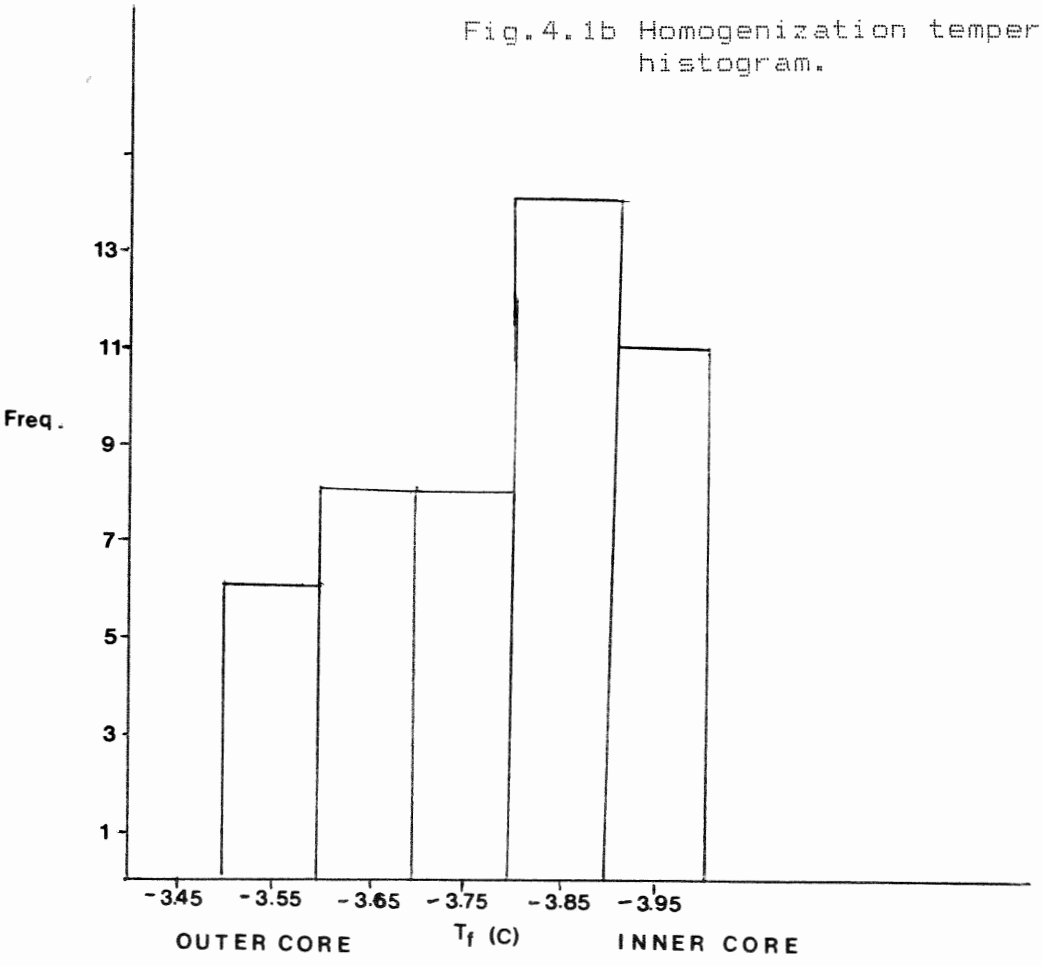

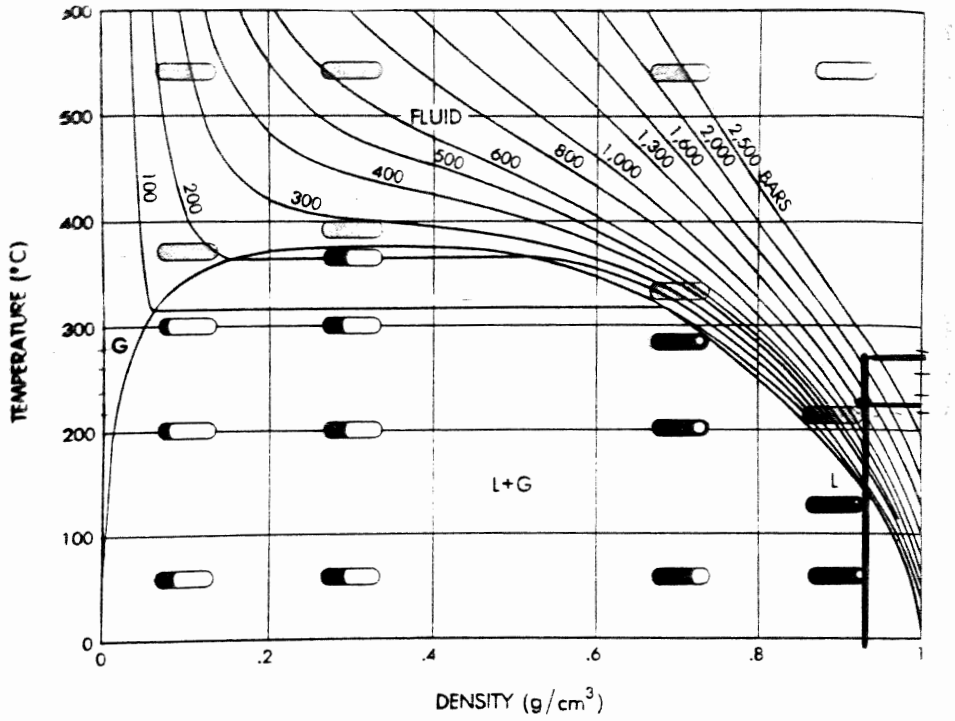

Roedder, 1984

Figure 4-5. Temperature-density diagram for the system H_2O, plotted from the data of Kennedy (1950b) and Maier and Franck (1966). The homogenization behavior of four inclusions, all trapped at 540°C (but at different pressures), is indicated. Liquid - black; gas - colorless; fluid - gray. The inclusions having density 0.9 and 0.7 homogenize in the liquid phase (L); that having density ~0.3 homogenizes at the critical point; that having density 0.1 homogenizes in the gas phase (G). Modified from Roedder (1972).

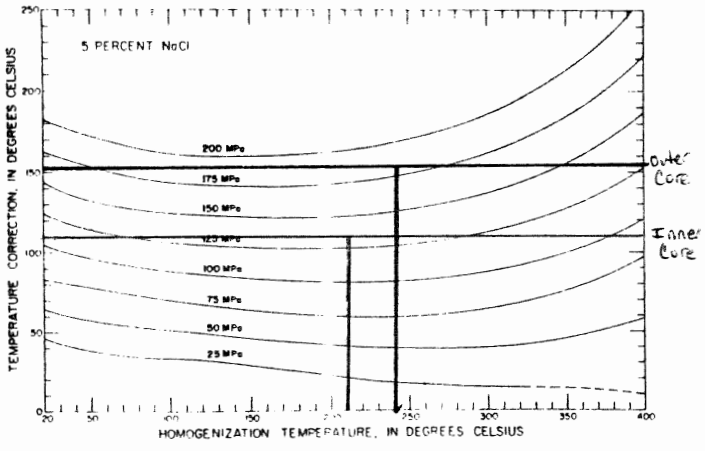

Figure "Pressure correction" for inclusions containing NaCl solutions of the weight percent NaCl indicated, as a function of Th and pressure in megapascals (i.e., bars x 0.1), from Potter (1977). Note - in the original publication, these diagrams are given in a larger format (each is 10 x 15 cm) that make for easier interpolation.

Fig. 4.6 Roedder, 1984

pressure change occurred during the evolution of the pegmatite, causing boiling to occur at a lower temperature in the inner core zone. The daughter minerals, however, do not dissolve when heated above 330°C in the liquid + vapour + solid inclusions, suggesting that pressure corrections are necessary. Such corrections mean that the T_hs, for 2- and 3-phase inclusions, are greater than 330°C, indicating that the inclusions formed at depth.

For the liquid + vapour inclusions, a T_h of 220°C and a fluid density of .9-.95 g/ml (based on the liquid/vapour ratio at room temperature) correspond to a pressure of ~1.3kb (Fig.4.3b). Using an average pressure of 1.2kb, the temperature correction for a T_h of 220°C is about 120°C, giving a pressure-corrected T_h of 340°C for the liquid + vapour inclusions (Fig.4.3c).

4.4 Vapour Bubbles and Daughter Minerals

In general, the vapour bubbles are single phase-features, and are composed mostly of water owing to the way in which they homogenize and freeze (Roedder,1984). Some of the bubbles in the negative crystal form inclusions (primary origin) are "double-bubbles", containing both liquid CO_2 and water vapour. This shows that the pegmatitic fluid contained CO_2 and H_2O.

The daughter minerals within the inclusions are impossible to identify by optical means, owing to the small size of the daughters, and because garnet is an isotropic mineral. Most of the daughter minerals have a pyramidal or cubic shape, suggesting that they are partial crystal forms of sylvite, or anhydrite (M. Zentilli, pers. comm.). Because the fluids in the inclusions have salinities below the

Fig.4.3 Roedder,1984

Table 8-2. Relation between depression of the freezing point Θ and wt% NaCl (W_S) [from equation (4) of Potter et al.(1978)].

Θ (°C)	W_S (Wt %)	Θ (°C)	W_S (Wt %)	Θ (°C)	W_S (Wt %)
0.000	0.000	7.000	10.508	14.000	17.893
1.000	1.698	8.000	11.728	15.000	18.767
2.000	3.343	9.000	12.886	16.000	19.606
3.000	4.922	10.000	13.985	17.000	20.412
4.000	6.430	11.000	15.032	18.000	21.189
5.000	7.862	12.000	16.029	19.000	21.939
6.000	9.221	13.000	16.982	20.000	22.663
				20.500	23.016

$$W_S = 0.00 + 1.76958\,\Theta - 4.2384 \times 10^{-2}\,\Theta^2 + 5.2778 \times 10^{-4}\,\Theta^3 [\pm 0.028].$$

$$\Theta = 0.00 + 0.581855\,W_S + 3.48896 \times 10^{-3} W_S^2 + 4.314 \times 10^{-4} W_S^3 [\pm 0.03°],$$

where Θ = the freezing point depression in °C, and W_S = the weight percent NaCl in solution. Table 8-2 gives a selected series of values derived from the second equation.

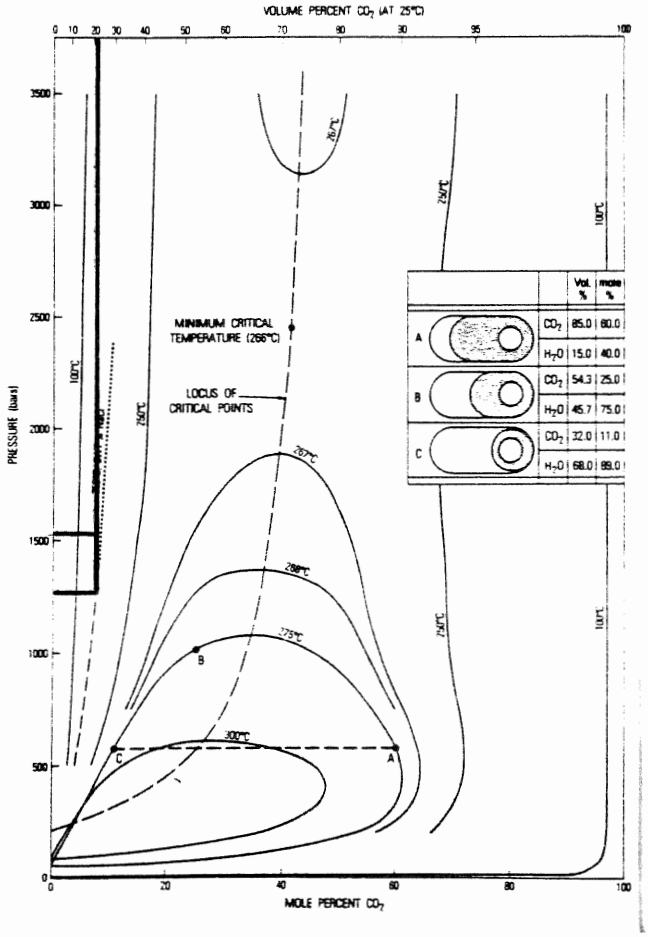

Fig.4.4 Roedder,1984

Figure [illegible]. P-X plot of isotherms showing compositions of coexisting phases in the system H_2O-CO_2, using data of Todheide and Franck (1963) and Greenwood and Barnes (1966). The upper abscissa shows volume percent CO_2 at 25°C along the CO_2 liquid-vapor curve (64 bars), assuming densities of CO_2 liquid, CO_2 vapor, and H_2O liquid of 0.71, 0.24, and 1.0 g/cm^3, respectively (Newitt et al., 1956; Keenan et al., 1969). The inset shows the two-dimensional appearance at the stated conditions for three cylindrical inclusions having compositions as given (liquid CO_2 shaded), which are also shown on the diagram. The 250°C isotherm for a 6 wt % NaCl solution from Takenouchi and Kennedy (1965b) is shown for comparison. From Roedder and Bodnar (1980).

saturation level(26%) with respect to NaCl, the daughter minerals cannot be solid NaCl (Roedder, 1984).

4.5 Conclusions

The following conclusions are evident from the fluid inclusion data:

1. Because the daughter minerals do not dissolve in the fluids when heated above 330°C, whereas the T_h for the liquid + vapour is 220°C, a large correction factor must be applied to compensate for the pressure effects (i.e because the garnet is out of static equilibrium).

2. The average CO_2 content of the inclusions is 20-25%. This means that an inclusion with a T_h of 220°C forms at about 1.5kb, or 4-5km beneath the earth's surface.

3. Based on an average pressure of 1.2kb, and a T_h of 220°C, a temperature correction of 120°C is necessary. Thus, the T_h is probably closer to 340°C for the liquid + vapour inclusions.

4. The average T_f or eutectic point for the fluid is -3.8°C. This temperature yields an average salinity of 6.3% for the liquid within a typical primary inclusion. This means that the fluid from which the garnet grew was only slightly saline, and that the daughter minerals in the inclusions are not NaCl.

5. The garnets **in the core** of the pegmatite are not magmatic, based on the low T_hs, and by implication none of the minerals adjacent to the garnets are magmatic either.

6. The presence of 1-, 2-, and 3-phase inclusions indicates that resurgent boiling occurred during the formation of the pegmatite.

7. The bimodality of the T_h histogram suggests the existence of a temperature gradient across the core of the pegmatite, and may also

record an abrupt pressure change during the emplacement of the pegmatite.

Chapter 5

Bulk-Rock Geochemistry

5.1 Introduction

Sections 5.2 to 5.5 present the major and trace element compositions of rocks from Units 1, 2, and 3, as determined by X-ray fluorescence techniques. Three samples from Unit 2, two samples from Unit 3, one sample from Unit 1, and one sample from an aplitic pod within the core of the main pegmatite. Unfortunately, the large grain size and the variations in mineralogy between zones made analysis of a representative sample of the pegmatite impossible.

5.2 Major and Trace Element Chemistry of Units 1, 2, and 3.

Units 1, 2, and 3 all have granitic bulk rock compositions (Table 5.2b). Close chemical similarities are apparent among all of the aplite samples, and between the granodiorite samples. Surprisingly, the monzogranite and the granodiorite samples are also chemically similar, and, therefore, the two units are discussed as one chemical entity.

The sample of the aplitic pod is compositionally intermediate between the aplites and the monzogranite and granodiorites.

The bulk rock compositions of the different units are summarized below:

a.Aplites: The major element compositions of rocks of Unit 2 compare very closely with that of a typical leucogranite (Table 5.2a, column WA1, WA2, WA3;Table 5.2b). The only major difference between the aplite and the leucogranite is that the aplite has a slightly higher Al_2O_3 content than the leucogranite. The chemical classification of the aplite as a leucogranite agrees with the mineralogical classification of

Table 5.2a WA=Aplite APP=Aplitic pod GD=Granodiorite MZ=Monzogranite

	WA1	WA2	WA3	APP	GD1	GD2	MZ1
SIO2	74.74	73.92	76.19	72.72	70.17	70.03	71.75
TIO2	0.08	0.08	0.04	0.20	0.37	0.38	0.25
AL2O3	14.85	14.67	14.42	15.11	15.53	15.62	14.96
FE2O3	0.39	0.69	0.15	1.73	2.35	2.46	1.74
FEO	nd	nd	nd	nd	nd	nd	nd
MNO	0.02	0.03	0.01	0.05	0.06	0.07	0.05
MGO	0.82	0.85	0.73	1.00	1.48	1.34	1.26
CAO	0.56	0.71	1.05	0.57	1.91	1.76	1.43
NA2O	2.99	2.76	4.34	3.86	3.95	4.10	4.04
K2O	5.26	5.29	3.31	4.96	2.94	2.82	2.88
H2O+	0.70	0.50	0.40	0.80	0.60	0.60	0.60
H2O-	nd	nd	nd	nd	nd	nd	nd
P2O5	0.14	0.26	0.14	0.14	0.20	0.19	0.22
TOTAL	100.55	99.76	100.78	101.14	99.56	99.37	99.18
Ba	280	317	161	472	446	353	294
Rb	164	155	98.00	251	127	125	124
Sr	72.00	63.00	77.00	79.00	155	137	108.00
Y	12.00	15.00	12.00	18.00	16.00	17.00	16.00
Zr	32.00	42.00	37.00	103.00	123	119	101.00
Nb	5.00	5.00	4.00	6.00	8.00	10.00	9.00
Th	nd	nd	nd	11.00	4.00	1.00	nd
Pb	24.00	18.00	10.00	21.00	8.00	6.00	7.00
Ga	14.00	15.00	13.00	13.00	17.00	19.00	18.00
Zn	16.00	25.00	11.00	56.00	50.00	57.00	50.00
Cu	nd	nd	nd	4.00	nd	nd	nd
Ni	1.00	1.00	3.00	6.00	5.00	5.00	6.00
V	2.00	3.00	nd	7.00	33.00	33.00	22.00
Cr	13.00	12.00	12.00	14.00	33.00	31.00	14.00

CIPW Norms

AN	6.87	7.30	10.43	5.55	19.89	18.03	14.43
Q	35.15	35.63	35.17	28.05	29.93	29.89	32.92
or	31.15	31.51	19.49	29.39	17.59	16.92	17.30
ab	25.35	23.54	36.59	32.75	33.85	35.21	34.74
an	1.86	1.83	4.27	1.92	8.28	7.60	5.75
C	4	4	2	3	3	3	3
hy	2	3	2	4	5	5	4
mt	0.2	0.3	0.1	0.8	1.1	1.2	0.8
il	0.2	0.2	0.1	0.4	0.7	0.7	0.5
ap	0.3	0.6	0.3	0.3	0.5	0.4	0.5

Table 5.2b Granitoid Compositions (after McBirney,1984)

	Granodiorite	Granite	Leucogranite
SiO_2	69.45	71.35	75.34
TiO_2	0.36	0.32	0.18
Al_2O_3	14.88	14.32	12.87
Fe_2O_3	1.59	2.00	0.25
FeO	1.23	0.65	0.80
MnO	0.07	0.09	0.09
MgO	1.24	0.97	0.41
CaO	2.81	2.26	0.81
Na_2O	3.69	3.71	3.88
K_2O	3.29	3.13	4.38
F	0.05	0.06	0.03

Unit 2 as a syenogranite.

b.Aplitic pods: The aplitic pods within the core of the main pegmatite are compositionally similar to true granites. They differ only in that the aplitic pods have a slightly lower (i.e. 2-3X) CaO contents and a much higher K_2O contents (Tables 5.2a, column APP;Table 5.2b).

c.Monzogranite & Granodiorite: Rocks of Unit 1 have a higher SiO_2, and lower Al_2O_3 and K_2O contents than those of Unit 3; otherwise these two units are almost identical chemically. Both are intermediate in composition between typical granites and typical granodiorites (Tables 5.2a & b). They differ from granite in having relatively low CaO contents, and high Al_2O_3 contents.

In general, these rocks are mineralogically and chemically similar to ones sampled by Douma (1988) and Clarke et al. (1980) from nearby outcrops.

5.3 Comparative Bulk Rock Chemistry

The following section presents brief comparisons of the chemistries of the aplites (Unit 2) to the monzogranites and granodiorites (Units 1 & 3), and of the aplitic pods to all three units.

a.Aplites: The aplites, especially samples WA1 and WA2, have significantly lower TiO_2, Al_2O_3, Fe_2O_3, MnO, MgO, and CaO, and higher SiO_2 and K_2O contents than rocks of Units 1 and 3. The aplites have much lower trace element concentrations than Units 1 and 3, except for a higher Pb content (Table 5.2a).

b.Aplitic pods compared with Units 1 & 2 & 3: The aplitic pods are compositionally intermediate between the aplites, and monzogranites and

granodiorites. Compared with these rocks the aplites have high Ba, Rb, Th, Pb, Zn, and intermediate Zr contents.

5.4 Two-Dimensional and Ternary Variation Diagrams

Two- and 3-variable discriminator diagrams were constructed using the data in Table 5.2a in order to determine whether the rock types are chemically the same, whether they are petrogenetically related, and whether they are related to the analyses of Douma (1988). Variables such as MgO vs CaO, TiO_2 vs MgO, K_2O vs CaO vs Na_2O, and Ti/(Y+Zr) vs Zr vs Y are plotted **only** because they show three distinct populations, as follows: a)aplites, b)monzogranites and granodiorites, and c)aplitic pod. The aplitic pod plots close to the monzogranites and granodiorites in the Ti/Y/Zr and MgO vs SiO_2 diagrams (Fig. 5.4a).

Generally, the binary diagrams also show that all three populations form approximate, straight-line trends, indicating that the three rock types may be genetically related and that they may originate from the same magma chamber. The plots also indicate that Units 2 (aplite) and 1 (monzogranite) may correspond to the same rock types analyzed by Douma (1988)(samples NPM538, 7NPM539).

5.5 Trace Element Analyses

Trace element data are plotted as chondrite-normalized spidergrams, but they are atypical because not all of the REEs were analyzed. More typical REE plots were generated from the data sets of both Douma (1988) and Clarke et al. (1980)(Fig. 5.5a-x). All of the analyzed samples have similar spidergram patterns, suggesting a common origin, or a similar post-petrogenetic history.

On the basis of trace element geochemistry, Clarke et al. (1980)

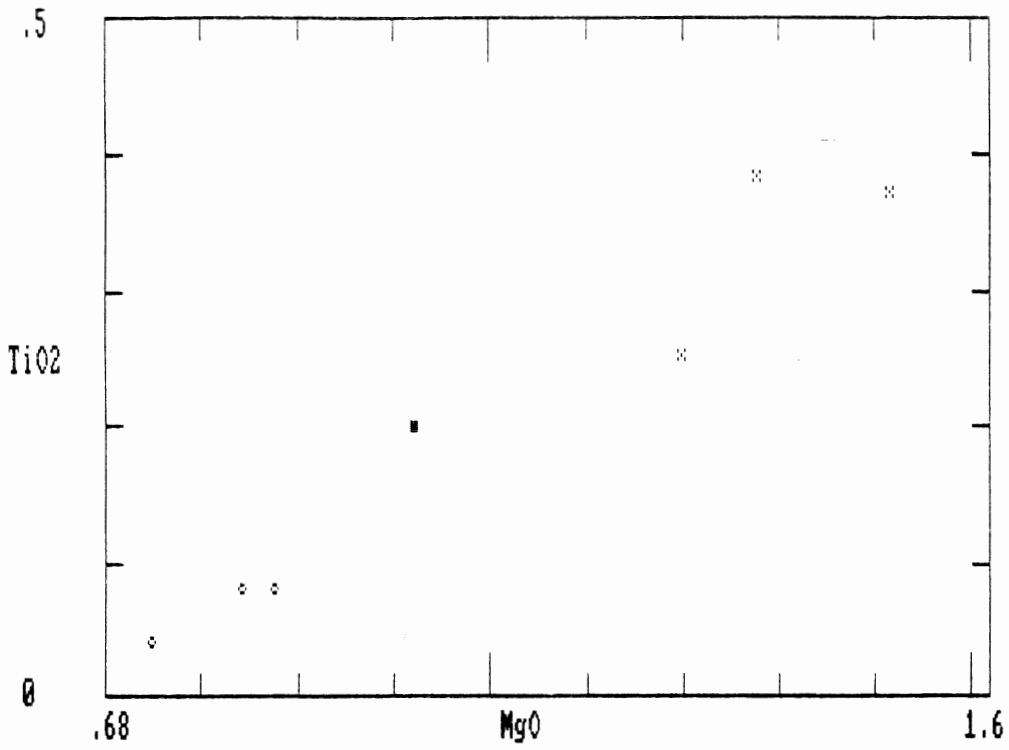

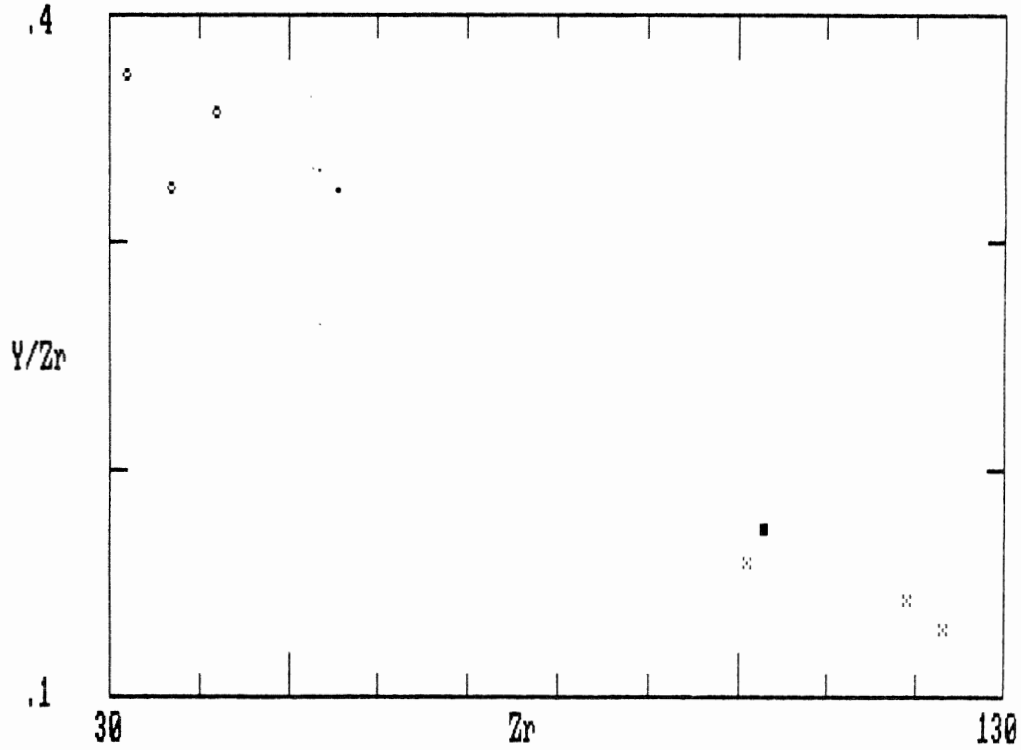

Fig.5.4a Binary and ternary variation diagrams
i) o = aplites, ■ = aplitic pods
⁘ = monzogranites + granodiorites

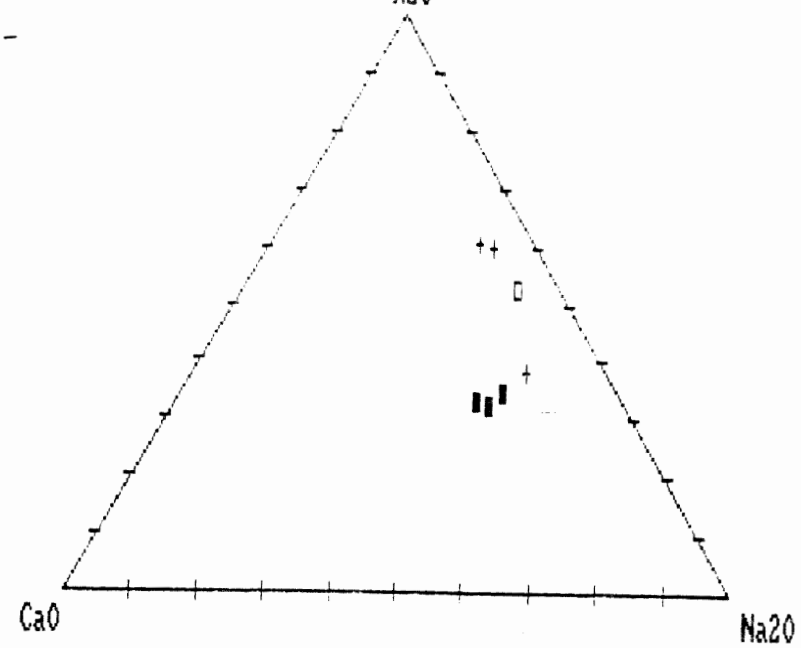

Fig.5.4a)ii + = aplites, ▯ = aplitic pod
■ = monzogranites + granodiorites

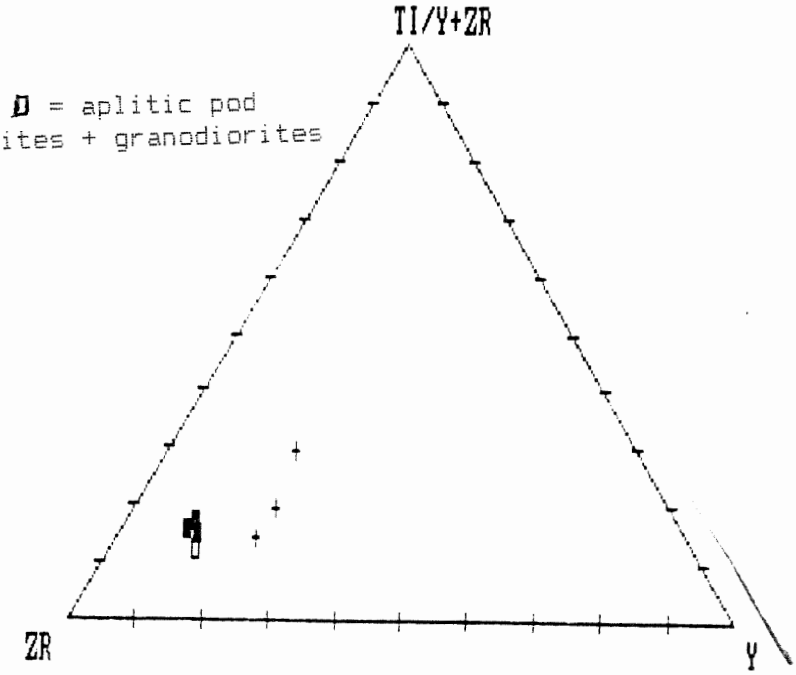

Fig 5.4 a i)

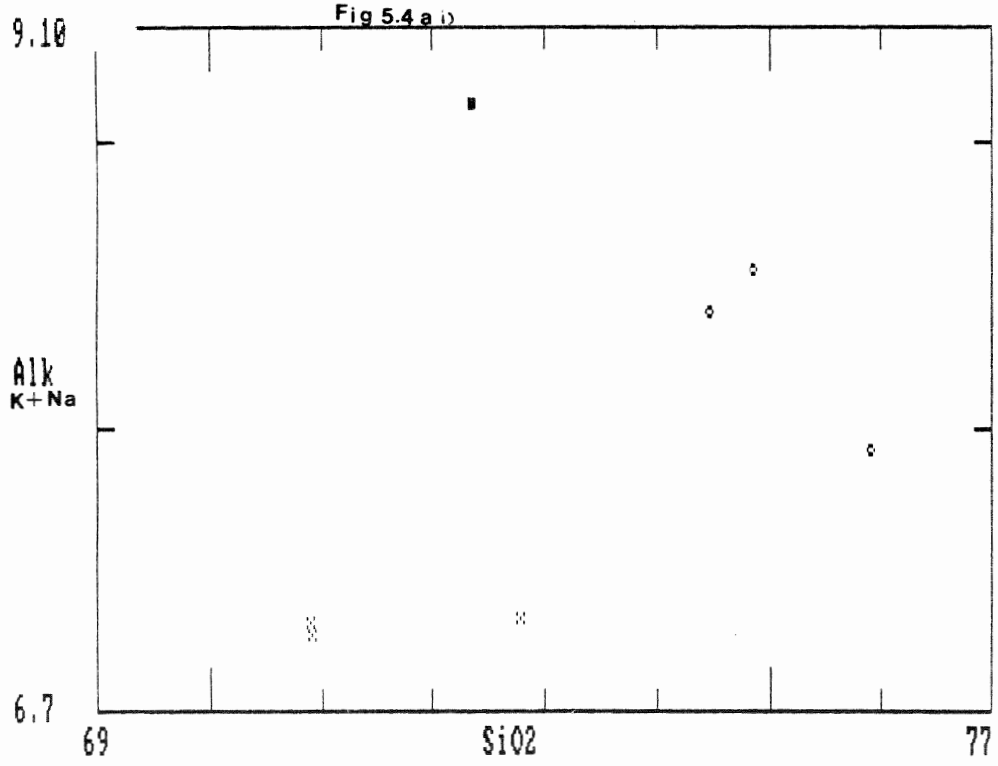

suggested that the granitoids of the Port Mouton pluton represent partial melts of either a metawacke-schist sequence in an orogenic belt, or of Precambrian gneisses. The presence of migmatites hosted by highly metamorphosed Meguma sediments several kilometres from Port Joli Harbour at Summerville Beach supports either type of origin, because migmatites are commonly associated with both orogenic belts and gneissic terranes. Clarke et al. (1988) suggest that the Meguma granitoids originate via melting of deeply buried gneisses or via partial melting of contaminated, mantle-derived material.

5.6 Conclusions

The geochemical evidence presented shows that:

1.Units 1, 2, 3, and the aplitic pods appear to have granodioritic, leucogranitic, granodioritic, and true granitic chemical characteristics, respectively.

2.The occurrence of corundum in the CIPW norm for all of the analyzed samples indicates that they are peraluminous.

3.All of the studied rock types have similar REE patterns, suggesting that they are derived from a common parent magma. Because the pegmatites are closely associated with these rock types, they probably originated from the same materials.

4.The REE patterns for rocks from the Port Mouton pluton suggest formation by partial melting of a metawacke-schist sequence(the Meguma), or of Precambrian gneisses (Clarke et al., 1980).

5.Units 1 and 2 correspond to the monzogranites and aplites analyzed by Douma (1988) from the same region, respectively.

10	11	12	13	14	
Musc.-Biotite Granodiorites		Musc.-Biotite Granites		Aplite	
72.10	73.25	70.02	72.74	73.42	SiO_2
.23	.22	.41	.19	.04	TiO_2
16.15	15.62	16.44	15.35	16.62	Al_2O_3
.31	.24	.19	.23	.36	Fe_2O_3
1.37	1.13	1.80	.97	1.11	FeO
.03	.03	.04	.04	.28	MnO
.33	.42	.71	.28	.10	MgO
1.36	1.33	1.68	.82	.52	CaO
3.82	3.79	3.66	3.65	4.31	Na_2O
3.54	3.52	4.17	3.97	3.08	K_2O
.06	.07	.13	.07	.06	P_2O_5
.83	.73	.67	.77	.40	H_2O^+
.08	.04	.05	.04	.02	H_2O^-
100.21	100.39	99.98	100.12	100.32	

Major element analyses for Port Mouton pluton (#10.11)

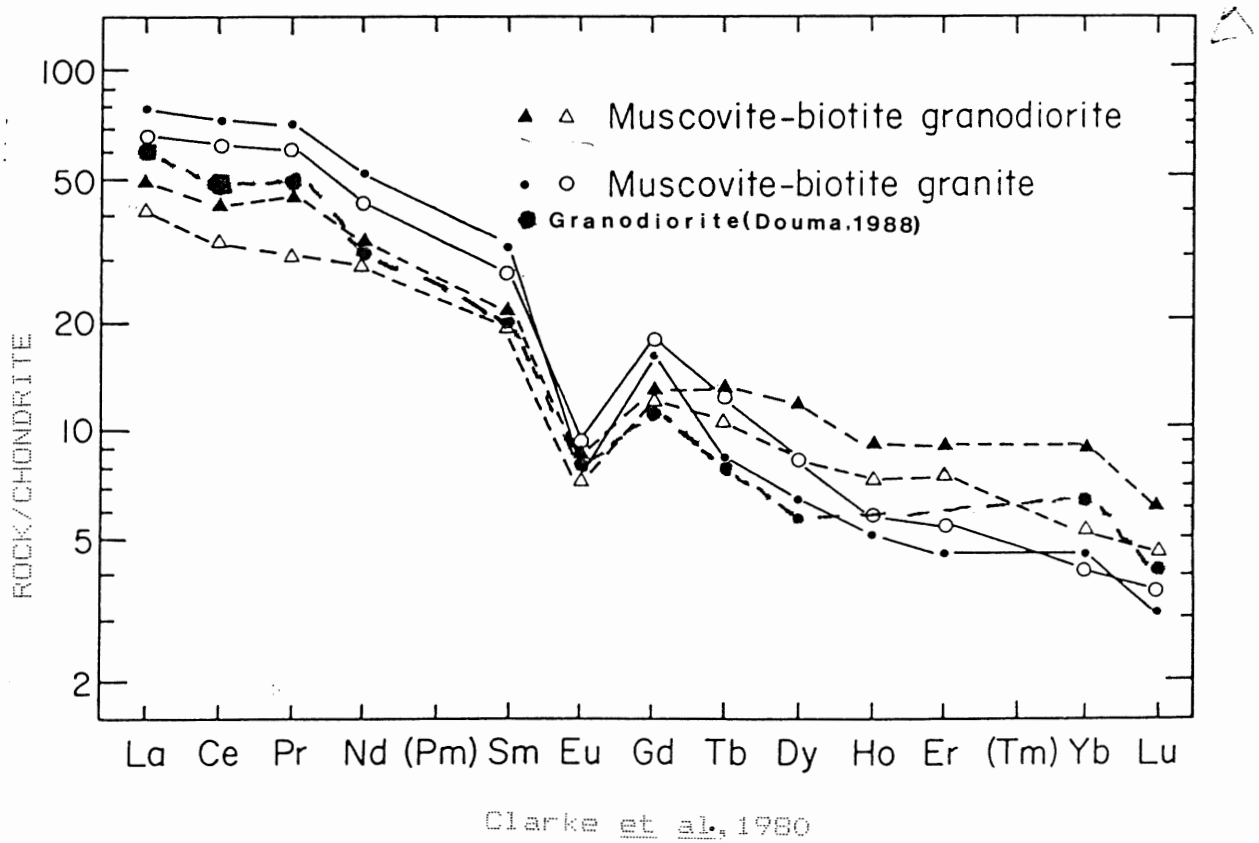

Clarke et al., 1980

Fig.5.5x REE abundance patterns for felsic rocks of the southern plutons

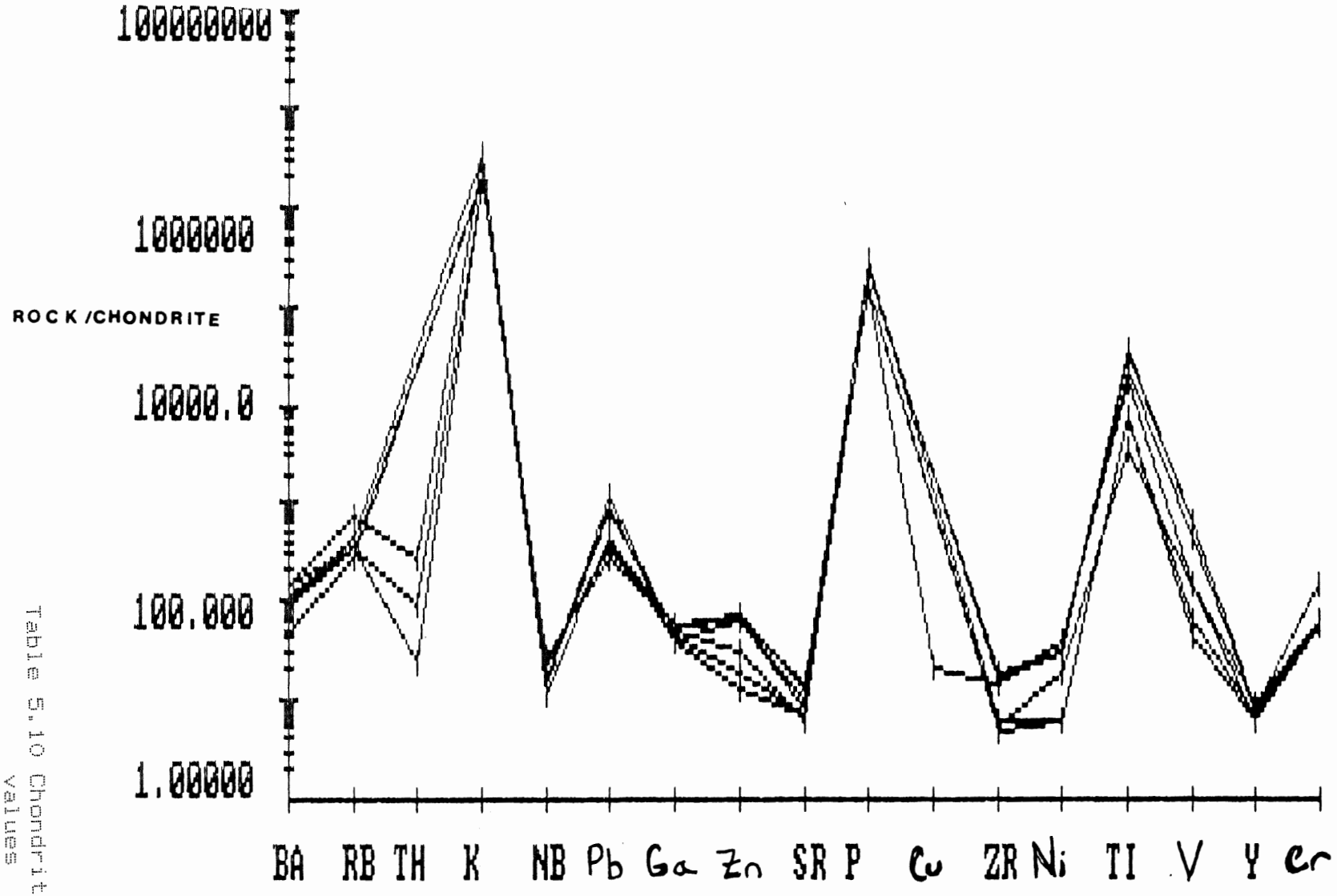

Fig.5.5a Trace element plots for all samples.
Trace element values normalized against chondrite values.

Table 5.10 Chondrite normalization values

La	0.329	Gd	0.276
Ce	0.865	Tb	0.0498
Pr	0.13	Dy	0.343
Nd	0.63	Ho	0.077
Sm	0.203	Er	0.225
Eu	0.077	Tm	0.0352

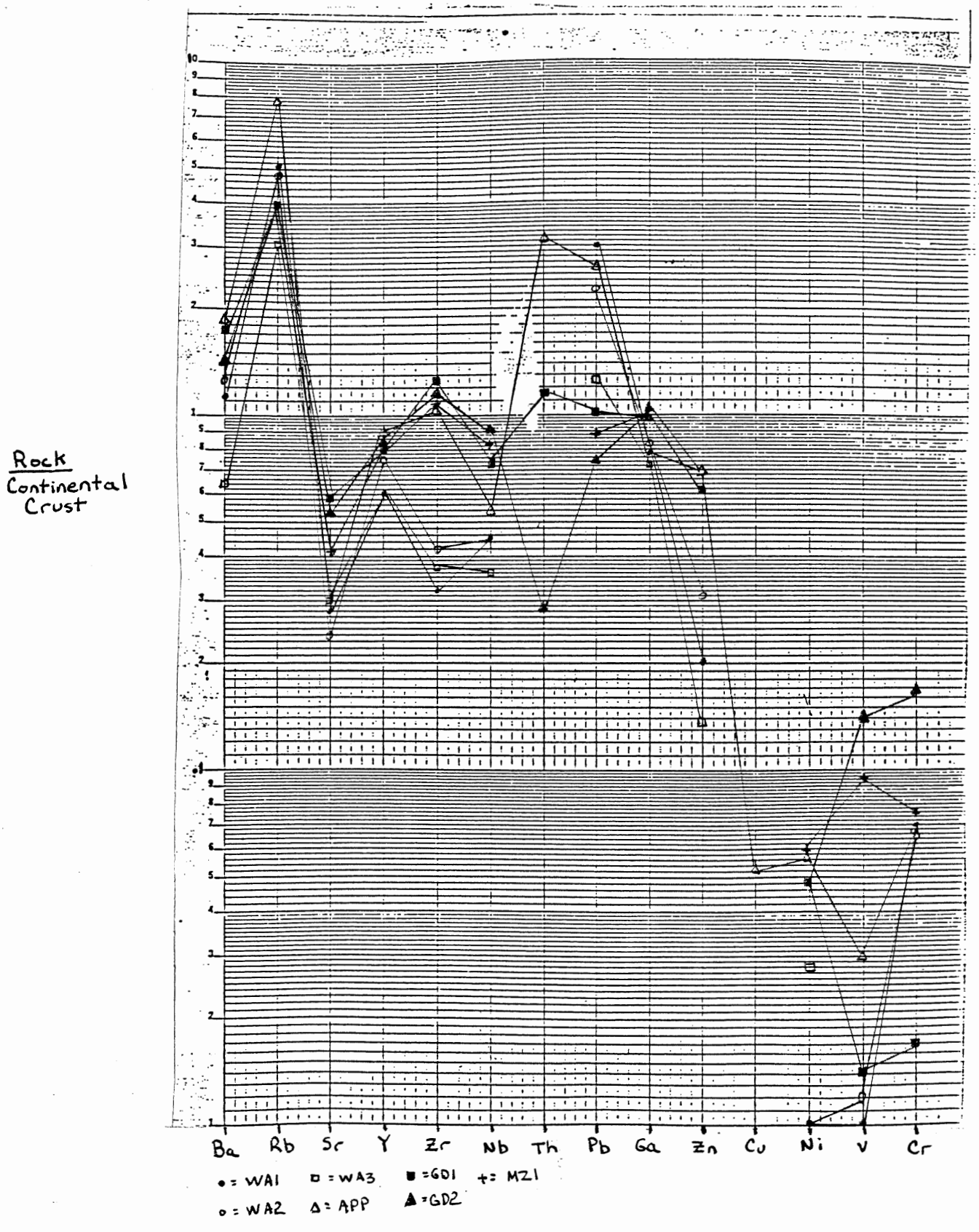

Fig. 5.5b Continental crust-normalized trace element plots.

Table 5.10b Continental crust normalization values.

;Li	13	Be	1.5	B	10	Na	2.3
;Mg	3.2	Al	8.41	Si	26.77	P	0.06
;K	0.91	Ca	5.29	Sc	30	Ti	0.54
;V	230	Cr	185	Mn	0.14	Fe	7.07
;Co	29	Ni	105	Cu	75	Zn	80
;Ga	18	Ge	1.6	As	1.0	Se	0.05
;Rb	32	Sr	260	Y	20	Zr	100
;Nb	11	Mo	1.0	Pd	0.001	Ag	0.08
;Cd	0.098	In	0.05	Sn	2.5	Sb	0.2
;Cs	1.0	Ba	250	La	16	Ce	33
;Pr	3.9	Nd	16	Sm	3.5	Eu	1.1
;Gd	3.3	Tb	0.6	Dy	3.7	Ho	0.78
;Er	2.2	Tm	0.32	Yb	2.2	Lu	0.3
;Hf	3.0	Ta	1.0	W	1.0	Re	0.0005
;Ir	0.0001	Au	0.003	Tl	0.036	Pb	8
;Th	3.5	U	0.91				

Chapter 6

Mineral Chemistry

6.1 Introduction

Sections 6.2 to 6.6 present microprobe and X-ray diffraction analyses of various minerals, particularly feldspars and garnets, from Units 1, 2, 3, and 4. The feldspars and garnets exhibit wide compositional variations that yield information about the processes acting during crystallization, and that may useful for constraining temperature and depth of crystallization.

6.2 Mineral Chemistry of Unit 1

Table 6.2a shows five of the 120 K-feldspar and plagioclase analyses and five structural formulae. The compositions of each of these minerals is discussed below:

a.Plagioclase: The unzoned plagioclase varies in composition from An_{22} to An_{34}, with an average of An_{27} (Fig.6.2a). The common zoned crystals vary from ~An_{40} in the cores to ~An_{25} on the rims. The lack of detectable Rb, Ba, or Sr in analyzed grains is unusual because these elements commonly substitute for Ca in the plagioclase lattice.

b.K-feldspar: The average composition of the K-feldspars is ~Or_{96}. Zonation of the K-feldspars is rarely greater than 4% in Or content across a crystal. The Ba and Rb contents of the K-feldspars are near zero in the main body of Unit 1, but they vary from 0.1-0.25 and 0.12-0.38 wt %, respectively, near contacts with pegmatite and aplite.

Table 6.2a Unit 1 Microprobe analyses and structural formulae

	Plag1	Plag2	Ksp1	Ksp2		Plag1	Plag2	Ksp1	Ksp2
SiO_2	64.95	64.50	65.55	65.71	Ca	0.17	0.18	.004	.004
TiO_2	0.03	0.00	0.05	0.07	Na	0.85	0.81	0.08	0.05
Al_2O_3	23.02	23.19	18.90	18.94	K	0.012	0.01	0.88	0.87
Cr_2O_3	0.06	0.06	0.09	0.06	Al	1.17	1.19	1.02	1.02
FeO	0.10	0.11	0.07	0.14	Si	2.81	2.80	2.99	2.99
NiO	0.00	0.00	0.00	0.00	O	8.00	8.00	8.00	8.00
MnO	0.00	0.11	0.08	0.10					
MgO	0.00	0.02	0.01	0.03					
CaO	3.60	3.92	0.09	0.09					
Na_2O	10.12	9.64	0.95	0.62					
K_2O	0.21	0.26	15.17	14.97					
Total	102.08	101.80	100.96	100.72					

Table 6.3a Unit 2 Microprobe analyses and structural formulae

	Plag1	Plag2	Ksp1	Ksp2		Plag1	Plag2	Ksp1	Ksp2
SiO_2	65.69	64.60	65.09	63.83	Ca	0.15	0.15	0	0
TiO_2	0.00	0.01	0.03	0.00	Na	0.63	0.84	0.06	0.08
Al_2O_3	23.29	23.10	19.53	19.49	K	.008	0.01	0.91	0.93
Cr_2O_3	0.00	0.03	0.00	0.07	Al	1.20	1.19	1.05	1.06
FeO	0.00	0.00	0.02	0.00	Si	2.86	2.81	2.97	2.95
NiO	0.00	0.00	0.00	0.00	O	8.00	8.00	8.00	8.00
MnO	0.00	0.01	0.00	0.00					
MgO	0.00	0.00	0.00	0.00					
CaO	3.36	3.28	0.01	0.02					
Na_2O	7.41	9.89	0.67	0.90					
K_2O	0.15	0.24	15.61	15.93					
Total	99.88	101.17	100.95	100.24					

Table 6.4a Unit 3 Microprobe analyses and structural formulae

	Plag1	Plag2	Ksp1	Ksp2		Plag1	Plag2	Ksp1	Ksp2
SiO_2	64.00	64.40	65.09	64.73	Ca	0.17	0.16	.003	.006
TiO_2	0.06	0.04	0.07	0.08	Na	0.80	0.82	0.07	0.07
Al_2O_3	22.51	22.50	18.71	19.00	K	.007	0.01	0.89	0.91
Cr_2O_3	0.07	0.06	0.09	0.08	Al	1.17	1.17	1.01	1.03
FeO	0.11	0.14	0.14	0.14	Si	2.82	2.83	2.99	2.97
NiO	0.00	0.00	0.00	0.00	O	8.00	8.00	8.00	8.00
MnO	0.10	0.00	0.00	0.13					
MgO	0.02	0.02	0.03	0.00					
CaO	3.77	3.41	0.06	0.12					
Na_2O	9.35	9.62	0.88	0.77					
K_2O	0.14	0.20	15.26	15.48					
Total	100.13	100.37	100.32	100.54					

6.3 Mineral Chemistry of Unit 2

Table 6.3 shows four of the 100 plagioclases and K-feldspars analyzed for major element, Rb, Sr and Ba contents. Typical results are as follows:

a. Plagioclase: Plagioclases from the aplite vary from An_{20-30}, and exhibit much less zoning than plagioclases from the monzogranites. Rb and Ba contents average about 0.7 wt% each, but the Sr is below the limit of detection.

b.K-feldspar: The K-feldspar in Unit 2 varies from Or_{91-96}, and is the largest variation for any unit. The Rb and Ba contents vary from 0.09-0.15 wt % and 0.08-0.21 wt %, respectively, but Sr remains below the detection limit of the microprobe.

c.Garnets:Garnets in the aplite are compositionally similar to the garnets in the main pegmatite (Section 6.5).

6.4 Mineral Chemistry of Unit 3

Table 6.4a presents four of approximately 50 analyses each of plagioclase and K-feldspar. A brief discussion of these minerals follows:

a.Plagioclase: The plagioclase varies in composition from An_{27} to An_{47}, and averages An_{36}. The Sr is below the detection level even though the Ca content is high. Barium and rubidium are also below the limit of detection in most of the plagioclase grains.

b.K-feldspar: The K-feldspar varies from Or_{92-96}, and averages Or_{94}. As for the other rock types, no Sr is detected in the feldspars. The Rb and Ba contents of these feldspars, 0.10-0.34 and 0.12-0.27 wt%, respectively, are similar to the feldspars from the monzogranites.

Figures 6.5g and h present the variations in feldspar compositions in each unit.

6.5 Mineral Chemistry of the Main Pegmatite

Table 6.5a presents some of the analyses of quartz, plagioclase, K-feldspar, and garnet in the pegmatite.

a.Quartz: Although the quartz is mostly SiO_2, it contains trace amounts of Al, Fe and Rb. The Rb content in quartz reaches a maximum of about .32 wt % in some cases, and is highest in samples from the core of the pegmatite. Martin (1982) suggests that such impurities are common, and that the replacement of oxygen by OH groups maintains electrical neutrality. The presence of such anions may account for the low totals of the quartz analyses.

b.Plagioclase: The plagioclase ranges from An_{3-27} at the border to An_{7-26} in the core zone, and averages An_8. There is no systematic variation in plagioclase composition across the pegmatite, and the plagioclase lacks detectable Ba, Rb, or Sr. Some plagioclases contain low levels (0.1-0.2 wt%) of Fe and Mn.

X-ray diffraction studies show that most of the plagioclase in the pegmatite is low albite to Na-intermediate albite, i.e. most of the Al is located in the T_1O site, and is thus highly ordered (Fig. 6.5a). Most of the K-feldspar is perthitic, reflective of significant amounts of Ca and Na in the lattice.

c.K-feldspar: The K-feldspar varies across the pegmatite from Or_{95-99}. The Ba content decreases from 1.13 wt% in the core to 0.1 wt% in the border zones. The average Rb content of the K-feldspar is 0.17 wt %, is highest in the core zone (.24-.27 wt%) and lower at the border zones

Table 6.5a Pegmatite Microprobe analyses and structural formulae

	Plag1	Plag2	Ksp1	Ksp2		Plag1	Plag2	Ksp1	Ksp2
SiO_2	65.10	69.62	64.70	64.63	Ca	0.16	0.04	.006	.006
TiO_2	0.04	0.05	0.09	0.07	Na	0.81	0.86	0.07	0.09
Al_2O_3	23.02	20.49	19.00	19.14	K	.004	.003	0.90	0.87
Cr_2O_3	0.00	0.00	0.00	0.00	Al	1.18	1.04	1.03	1.04
FeO	0.11	0.13	0.16	0.19	Si	2.83	2.98	2.97	2.97
NiO	0.00	0.00	0.00	0.00	O	8.00	8.00	8.00	8.00
MnO	0.00	0.00	0.03	0.00					
MgO	0.03	0.02	0.03	0.04					
CaO	3.47	0.79	0.13	0.13					
Na_2O	9.58	10.34	0.78	1.10					
K_2O	0.08	0.06	15.40	14.79					
Total	101.43	101.51	100.66	100.48					
	Border Zone	Core Zone	Border Zone	Core Zone					

Table 6.5a Pegmatite Microprobe analyses and structural formulae

	Garnet1	Garnet2		Garnet1	Garnet 2
SiO_2	36.88	36.13	Ca	0.02	0.03
TiO_2	0.00	0.04	Fe	1.77	1.67
Al_2O_3	20.74	20.35	Mg	0.14	0.12
Cr_2O_3	0.00	0.00	Mn	1.07	1.24
FeO	25.95	24.17	Al	1.99	1.98
NiO	0.00	0.00	Cr	0.00	0.00
MnO	15.49	17.75	Ti	0.00	0.00
MgO	1.14	0.99	Si	3.00	2.98
CaO	0.28	0.33	O	12.00	12.00
Na_2O	0.08	0.11			
K_2O	0.00	0.00			
Total	100.57	99.86			
	Border Zone	Core Zone			

Fig.6.5e Typical garnet analyses rare-element pegmatites

	1.	2.
SiO_2	33.36	35.70
TiO_2	-	-
Al_2O_3	14.99	19.22
Cr_2O_3	-	-
FeO	2.51	28.35
NiO	-	-
MnO	43.10	15.32
MgO	-	0.27
CaO	1.10	0.26
Na_2O	0.21	-
K_2O	-	0.04

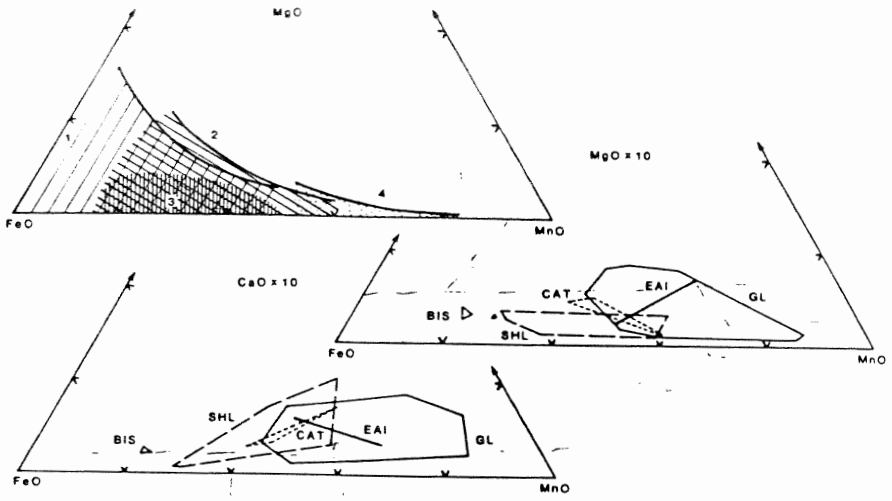

Fig.6.5f Cerny,1982

FIG. Compositional fields of garnet from different pegmatite types; A - northern Karelia (Salye 1975): 1 - muscovite formation A, 2 - muscovite formation B, 3 - muscovite + rare-metal formation, 4 - rare-element formation; B and C - Winnipeg River district, Manitoba (Černý et al. 1981): diverse pegmatite groups of a complex rare-element district.

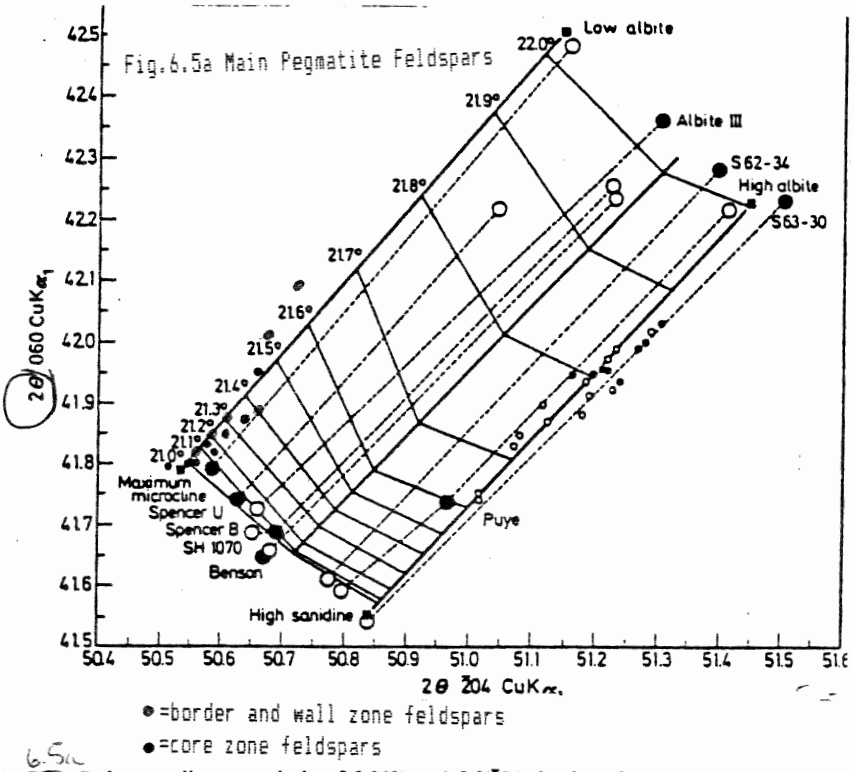

Other typical values from XRD patterns

Trial	2θ values for 060	$\bar{2}$04	$\bar{2}$01
1	41.85	50.61	21.29
2	41.88	50.65	21.16
3	42.20	50.71	21.38
4	42.07	50.76	21.30
5	41.82	50.70	21.24
6	41.84	50.56	21.15
7	41.85	50.57	21.05

6.5a

Fig. 6.5a. Reference diagram relating $2\theta(060)$ and $2\theta(\bar{2}04)$ in the "three-peak" method of Wright (1968). The four solid squares show reference points for the extreme end-members, and the straight lines represent Orville's microcline and sanidine series and the orthoclase series of Wright and Stewart. The dashed lines show ion-exchange paths. Small circles show data for natural feldspars. The crossing contours show the expected values for $2\theta(\bar{2}01)$. This figure is analogous to Fig. 7-14b, whose legend provides further information. (From Wright, 1968. Fig. 3)

(0.18 wt%). Surprisingly, there is no correlation between the Rb_2O and K_2O or Na_2O (Fig.6.5b). This is unexpected, because Rb substitutes for alkalis in the K-feldspar lattice, and an inverse relationship between Rb_2O and Na_2O or K_2O is expected.

Martin (1982) suggests that the low Ca and Sr contents of the K-feldspars results from extreme crystal fractionation of Ca-bearing phases in the source region of the pegmatite. Thus, the system Ab-Or-Qz-H_2O approximates the mineralogy of the border and wall of the pegmatite better than a system involving pure end-member anorthite.

X-ray diffraction analyses show that most of K-feldspar in the pegmatite is almost maximum microcline, i.e. almost all the Al in the lattice is located in T_1O coordination sites. This agrees with the high degree of Al-Si ordering calculated for the plagioclases(Fig.6.5a). Insufficient data are available to determine whether the Al-Si ordering process in the feldspars was incremental or gradational during the cooling process, i.e. whether the ordering occurred in steps at discrete temperatures, or evenly at all temperatures.

d.Garnets: The garnets are intermediate in composition between almandine and spessartine. The almandine content of the garnets varies from about 58 mol % to 65 mol %(i.e Fe > Mn). An inverse relationship between the Fe and Mn contents within the garnets suggests that both are in the +2 oxidation state, and substitute for each other rather than for Al (Fig.6.5c,). There is also an inverse relationship between the Fe and Mn in garnets across the pegmatite; the Fe is highest at the borders, whereas the Mn is highest in the core zone (Fig. 6.5d). The garnets are very similar to those found in rare-element pegmatites, further suggesting emplacement of the pegmatite at depth (~10-12km)(Fig. 6.5f).

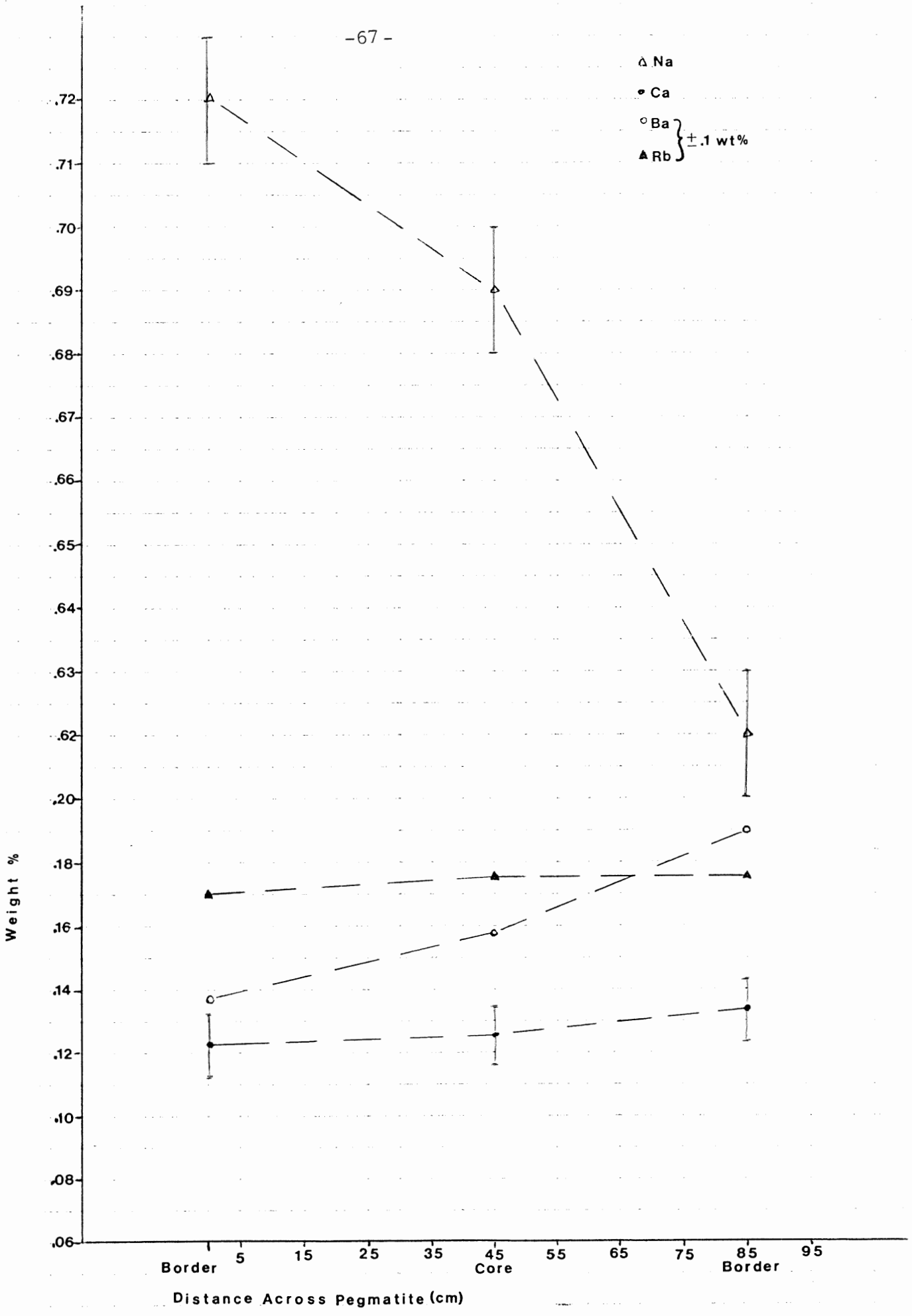

Fig. 6.5b Variation in feldspars across pegmatite.

Fig. 6.5d Mol fraction Fe vs mol fraction Mn in the cores of garnets from across the pegmatite, i.e. from the border and core zones of the main pegmatite.

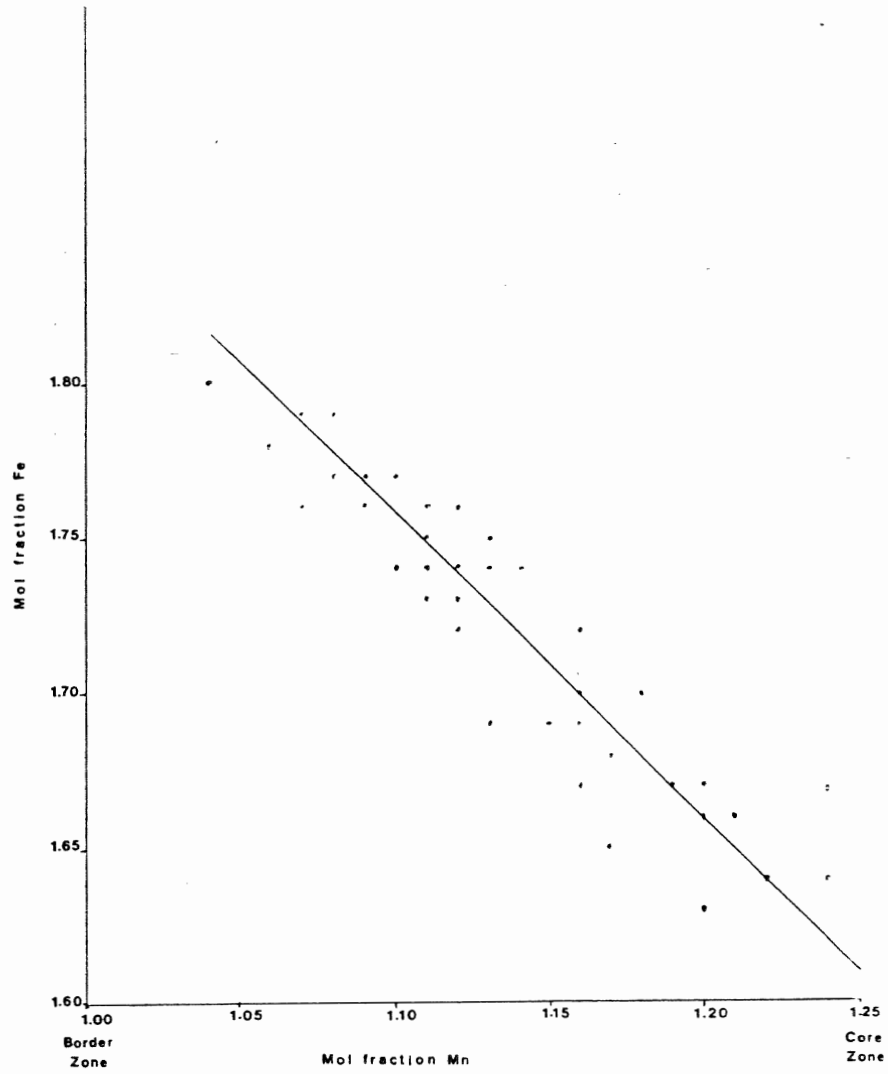

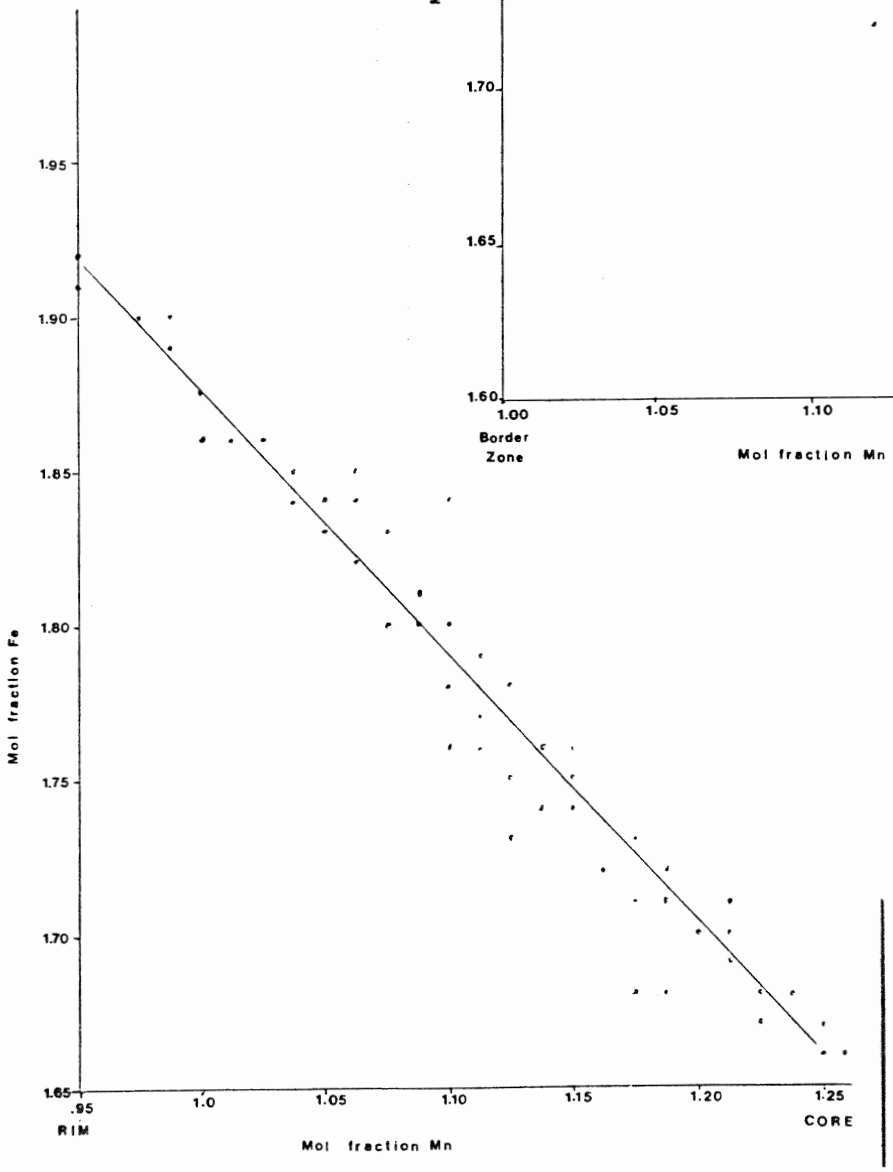

Fig. 6.5c Mol fraction Fe vs mol fraction Mn in zoned garnet crystals from the core of the main pegmatite only.

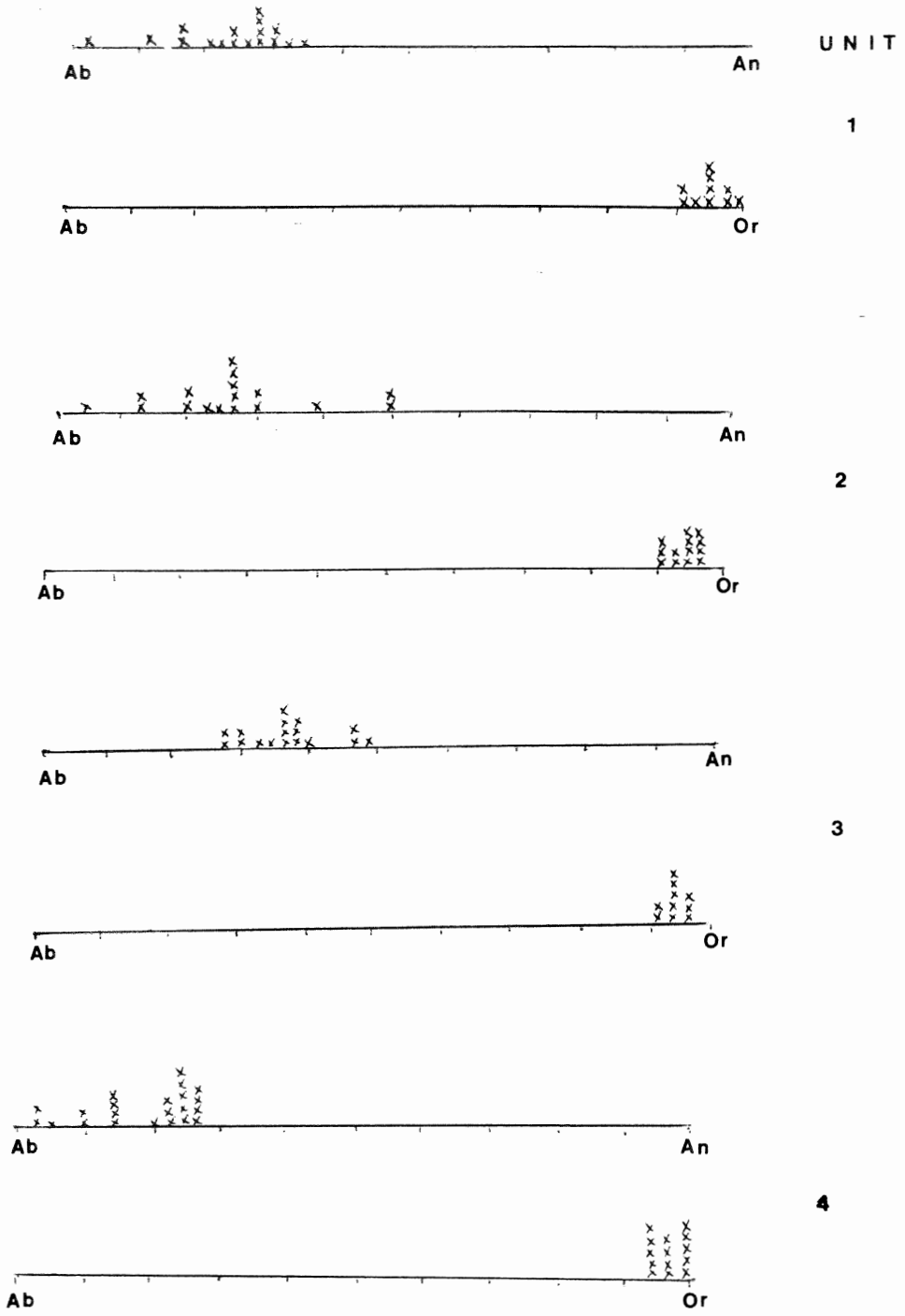

Fig6.5g Histograms of feldspar variation

Vertical Scale: x = 2 feldspars

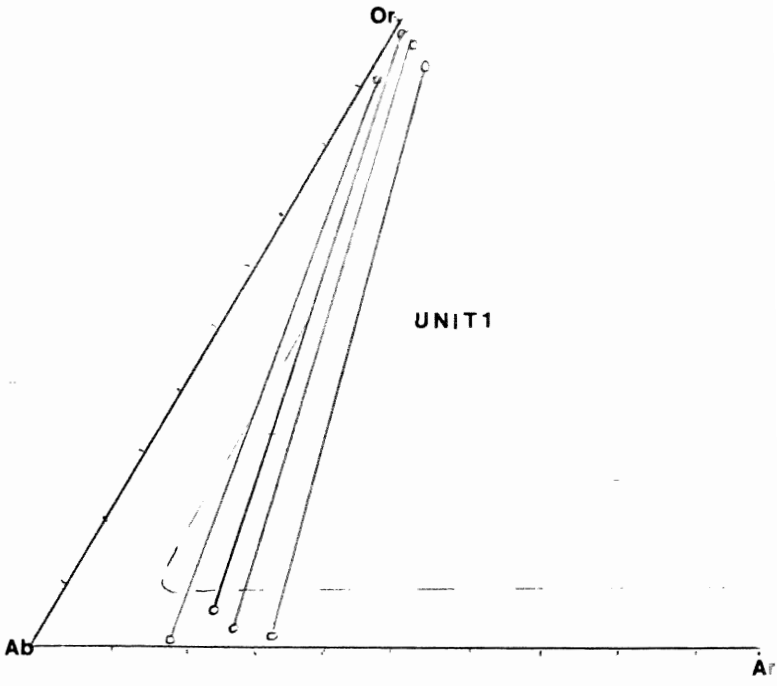

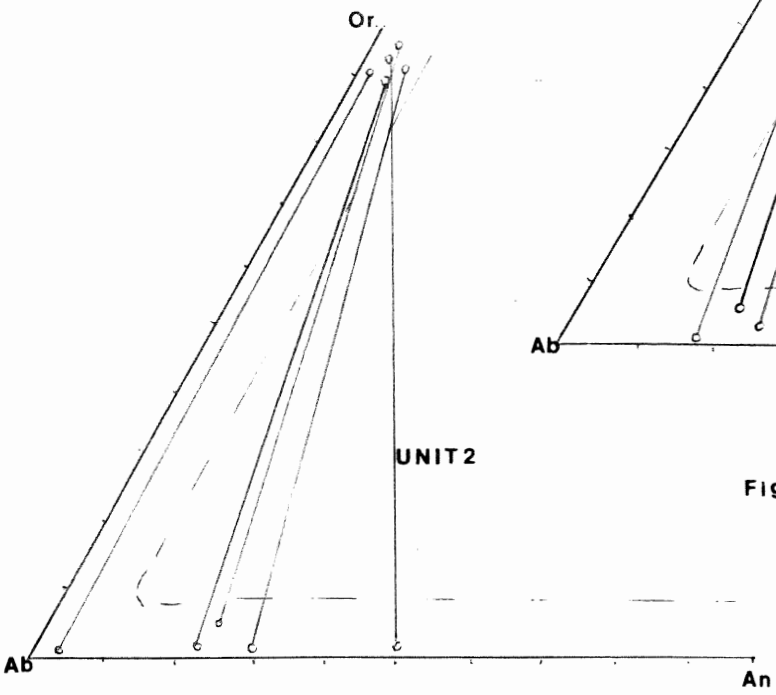

Fig 6.5h Coexisting feldspars

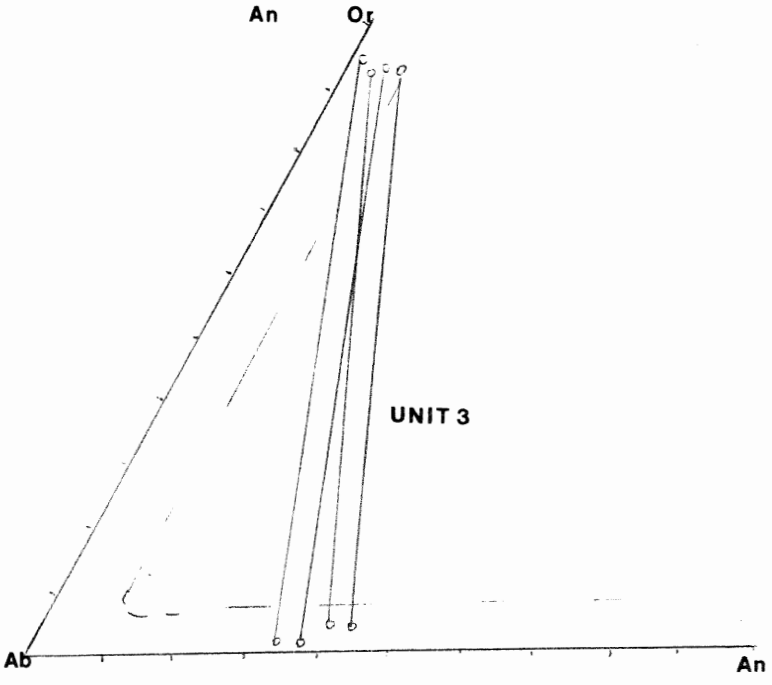

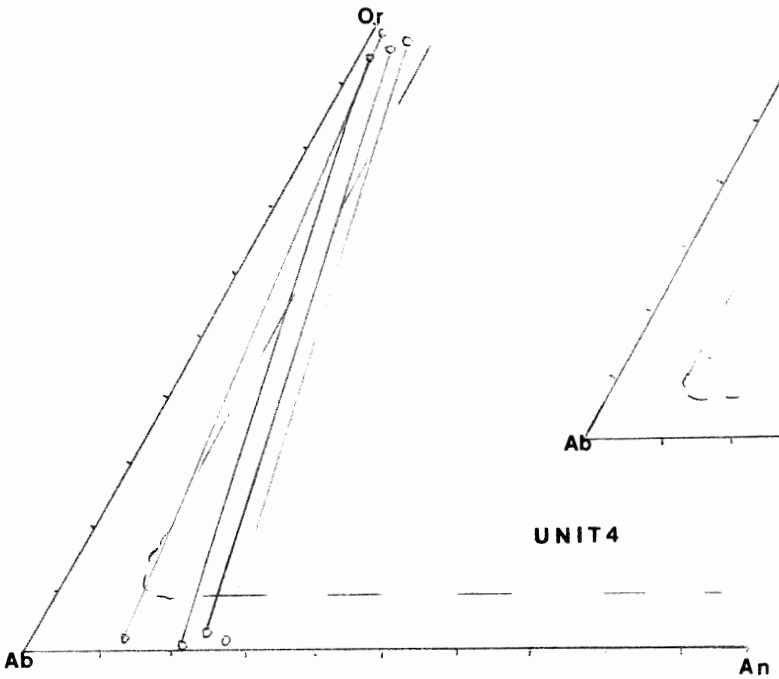

Emplacement of the pegmatite at 10-12 km contradicts the fluid inclusion results. The fluid inclusions record pressures of about 1.5 kb, corresponding to a depth of emplacement of 4-5 km.

6.6 Conclusions

The following conclusions are evident from the mineral composition data:

1.The garnets and feldspars in the main pegmatite chemically zoned.

2.The feldspar and garnet compositions are similar to those in rare-element pegmatites, suggesting a relatively deep origin, but not a great depth of emplacement (Section 6.5d).

3.The absence of detectable Sr from all rock types indicates extensive fractionation of Ca-rich phases during petrogenesis.

4.The presence of two coexisting feldspars and perthite, and the intergrowth of these phases with quartz in the wall and border zones of the pegmatite, indicate an origin from a Ca-poor, H_2O-rich granitic fluid crystallizing at depth (Cerny,1982).

5.Some temperature-controlled process, such as Rayleigh diffusion or disequilibrium growth, is responsible for the compositional variations of the garnets and feldspars.

6.A significant variation of Na content of the K-feldspar across the main pegmatite does not reflect variations in the overall Or content of the K-feldspars, suggesting that at least some of the Na is present as an impurity rather than as a substitution for K in the feldspars.

Chapter 7

Summary and Conclusions

7.1 Introduction

This chapter summarizes the main conclusions of previous chapters and presents several hypotheses for the origin of structural, chemical, and mineralogical zonation in the main pegmatite.

7.2 Summary of Main Conclusions

The major conclusions regarding the Wickwire pegmatite and the host rocks of the Port Mouton pluton are as follows:

1. The field relations indicate a geologic history for the host rocks and pegmatite as follows:

Youngest: Weathering of the pegmatite

Uplift and erosion

Possible fluid overprinting during intrusion of pegmatite

Late aplites and pegmatites intruded

Granodiorite intruded

Aplites intruded

Monzogranite intruded

Burial, deformation and partial melting of Meguma sediments

Oldest: Meguma sediments deposited

2. Rubidium-strontium dating methods yield an age of 340 $\pm$ 23 m.y. for the Port Mouton pluton (Keppie & Smith,1978)(Fig.7.1). If this age is correct, the Port Mouton pluton could be associated with the intrusion of the South Mountain batholith.

3. The rock types hosting the pegmatite are peraluminous, supporting

the hypothesis that the Port Mouton pluton originated from metasedimentary source rocks.

4. The repetitive nature of intrusions in the Port Mouton region, i.e. mafic(mzg)-felsic(apl)-mafic(gd)-felsic(apl+peg), indicates three cycles of intrusion (Douma,1988). It is unexpected that, if the monzogranite and granodiorite are genetically related, the granodiorite should evolve from the less mafic monzogranite. This reverse zonation may result from the separation and stratification of felsic magmas above mafic magmas in a given chamber. The felsic magma is intruded first, followed by a mafic intrusion, giving the appearance that the mafic magma evolved from the felsic magma.

5. Quartz in all the rock types shows some degree of deformation. This deformation decreases away from the wall zone of the pegmatite, suggesting that the strain was generated by the intrusion of the pegmatite and/or fracturing associated with the intrusion.

6. The similarity between the monzogranite and granodiorite compositions, REE patterns for the monzogranites, aplites, and granodiorites, and the association of the monzogranites, aplites, granodiorites, and pegmatites all suggest close temporal, spatial, and probable genetic relationships between the monzogranites, aplites, and granodiorites (Douma,1988).

7. The REE spidergrams for the monzogranites, aplites, and granodiorites suggests an origin from deeply buried Precambrian gneisses or from an orogenic metawacke-schist belt (Clarke et al.,1980). The presence of migmatites and associated pegmatites several kilometres from the study area supports such an origin.

8. The main pegmatite is granitic in composition and coarse-grained.

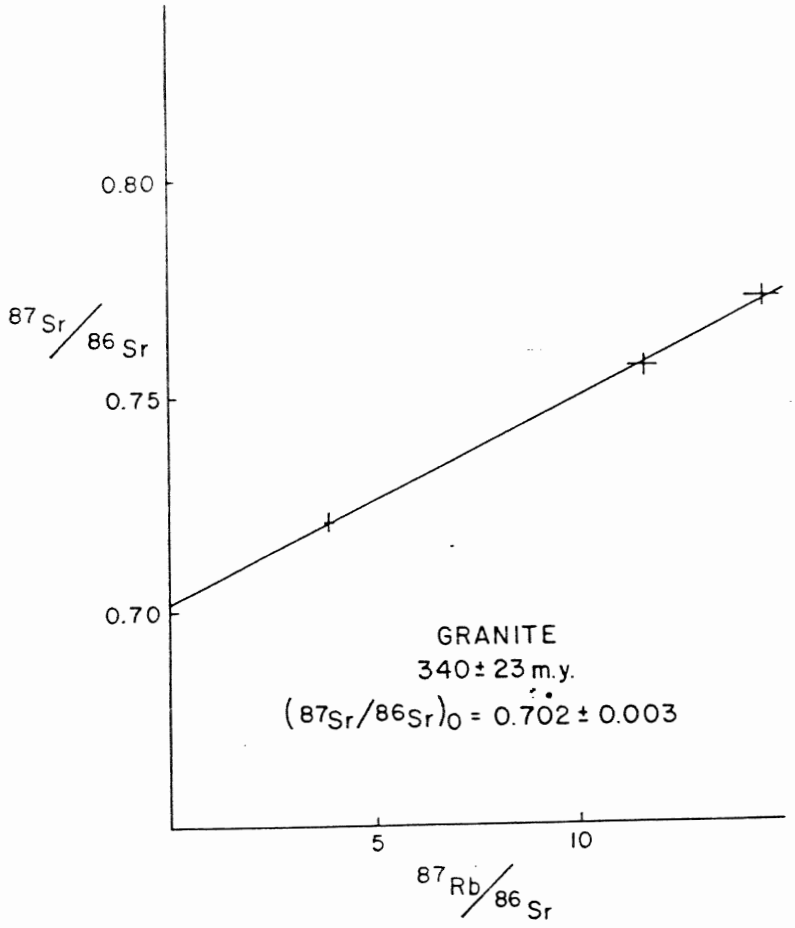

Fig.7.1 Age dating Port Mouton Pluton Keppie & Smith,1978

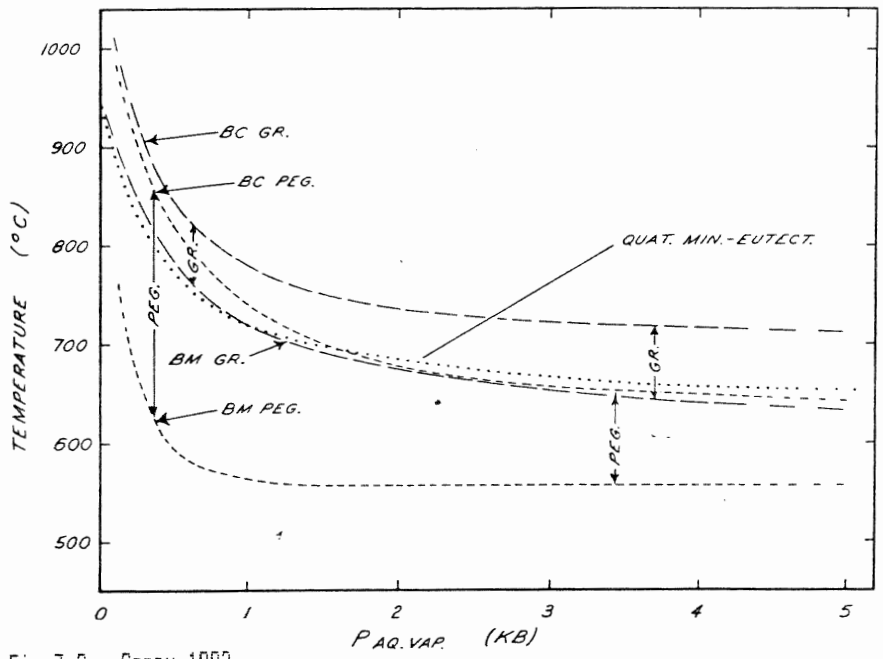

Fig.7.2 Cerny,1982

Fig. Experimentally determined relationships between confining pressure of aqueous vapor and temperatures of beginning of crystallization (BC) and beginning of melting (BM) for Stone Mountain, Georgia granite (GR. and long-dash curves) and for Harding, New Mexico pegmatite (PEG. and short-dash curves). Each pair of curves defines maximum temperature ranges of isobaric crystallization for the corresponding vapor-saturated rock - water system (see double-barbed arrows). Relationships for the haplogranite system $NaAlSi_3O_8$ - $KAlSi_3O_8$ - SiO_2 - H_2O are shown for comparison (dotted curve). Based on data from C.W. Burnham, P.M. Fenn, R.H. Jahns, W.C. Luth, R.F. Martin, J.C. Steiner, and O.F. Tuttle.

Generally, the main pegmatite fits the definition of a granitic pegmatite presented in the first chapter.

9. The pegmatites are traceable from the main body of aplite (Unit 2a), suggesting that the pegmatites are late stage differentiates of these aplites.

10. The pegmatite is parallel to contacts within the banded aplites, and semi-parallel to the flow foliation in Units 1 and 3, suggesting that the intrusion of the main pegmatite is fracture controlled.

11. The main pegmatite exhibits mineralogical, structural and chemical zonation, as shown by petrographic examination, field relations, and microprobe analyses, respectively(Chapters 1, 2, and 5).

12. The garnet and feldspar compositions in the main pegmatite are similar to those in other pegmatites suspected of having a relatively deep (7-10 km) origin (Chapter 6).

13. The low Ca and Sr contents of the feldspars indicate that the pegmatite originated via a high degree of fractionation of Ca-bearing phases at depth (Cerny,1982).

14. Furthermore, the presence of maximum microcline in all zones of the pegmatite suggests that the dyke cooled over a long time, consistent with injection at great depth.

15. The crystallization temperature in the core of the pegmatite estimated from fluid inclusions is at least 250°C. The presence of highly insoluble daughter minerals within inclusions indicates that this temperature is lower than the <u>in situ</u> crystallization temperature. The inclusions freeze at relatively high temperatures indicating that: a)the fluid from which the pegmatite crystallized was not highly saline, and b)the daughter minerals are silicates or halide compounds, such as

FIG. 1. Diagrammatic outline of model for the derivation of water-saturated granitic magmas (with or without other volatile constituents) and for the crystallization of pegmatites and related rocks. The following processes are indicated by circled letters:

A—Mechanical emplacement of magma or rest-magma containing some water.
B—Segregation of water-bearing rest-magma within a crystallizing igneous body.
C—Partial melting of crustal material *in situ* and in the presence of some water.
D—Crystallization of anhydrous minerals, with or without reaction between solid phases and silicate melt, + Process A + Process B.
E—Crystallization of anhydrous minerals, with or without reaction between solid phases and silicate melt.
F—Reduction in total confining pressure on the system.
G—"Osmotic" separation of water from the silicate melt.
H—Partial escape of aqueous fluid from the host body of silicate melt, with movement of materials by and through the fluid phase.
I—Marked reduction in total confining pressure on the system, with attendant "quench" crystallization.
J—Crystallization from silicate melt and aqueous fluid, with or without reaction between solid phases and the fluid phases, + Process A.
K—Partitioning of nonvolatile constituents between silicate melt and increasing amounts of aqueous fluid, with diffusion of materials along concentration gradients, especially in the aqueous phase; crystallization from both fluid phases, segregation of solid products according to amount and degree of interconnection of the aqueous fluid, and reaction between solid phases and the fluid phases.
L—Crystallization from aqueous fluid or fluids (and possibly, in rare instances, from some residual melt), with reaction among solid and fluid phases, exsolution of solid phases with diffusive transfer of materials over a wide range of scales, and development of mineral assemblages stable at relatively low temperatures.
X—Crystallization from silicate melt, with or without reaction between solid phases and the liquid, followed in late or very late stages by Process K or by Processes K and L.

The final products, which are interrelated and commonly intergradational, can be identified as follows:

I—Pegmatite, hybrid rocks with pegmatitic material, mineral impregnations, and other products of metasomatic alteration of country rocks.
II—Granite with miaroles, small amounts of autoinjection pegmatite, interstitial aplitic material, or interstitial analogues of the reaction and replacement products of Process L.
III—Pegmatite with or without aplite, the following spectrum of rock types in general representing a range from relatively small to relatively large amounts of aqueous fluid in the systems:

1. Very coarsely porphyritic pegmatite, granite, or aplite, or combinations thereof.
2. Pegmatite with clusters, pods, and lenses of very coarse-grained to giant-textured material.
3. Pegmatite with marked distribution of minerals, generally with sodic, fine-grained to aplitic groundmass constituents.
4. Pegmatite with markedly asymmetric zonal distribution of minerals, commonly with well-defined masses of sodic aplite.

IV—Pegmatites and pegmatitic rocks as in III above, but with more abundant and widespread features ascribable to corrosion and mineral replacement, together with hydrothermal minerals formed at relatively low temperatures.
V—Aplite, with or without masses of pegmatite.

KEY to Fig 7.3

Jahns & Burnham, 1969

Possible paths for the Wickwire pegmatite:
C-F-K
C-F-J-K

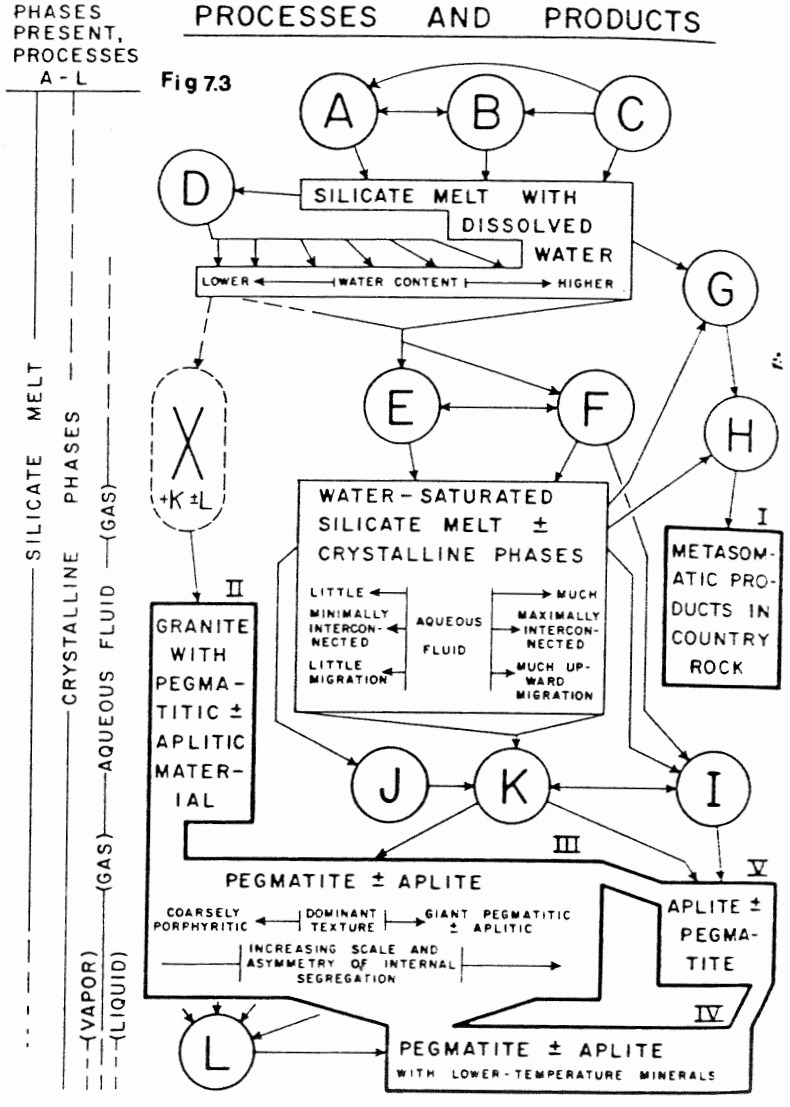

fluorite.

16. The main pegmatite has a dual origin; the border and wall zones are of an igneous origin, whereas the core region is of a hydrothermal origin. The mineralogical, structural, and chemical zonation in the main pegmatite result from such a dual origin, supported by the textures of quartz, garnet, and beryl in the core and border zones (Chapter 3).

17. The aplitic pods in the geometric (not zonational) core of the main pegmatite are not replacement bodies, but rather some kind of fracture filling because they are neither vertically nor horizontally extensive, and have no specific orientation with respect to the zones of the pegmatite. The aplitic pods may only be complex inclusions.

18. The increasing grain size (i.e. gradational increase within a zone, incremental increase across zone boundaries) and lack of chill zones toward the core of the main pegmatite suggests that whatever the nature of the two-fold origin, there was no significant gap in time between the termination of one mechanism and the initiation of the next.

7.3 Genetic Models for the Wickwire Pegmatite

Several existing models may explain the chemical, mineralogical, and structural features of the main pegmatite. Each model must explain the following features of the pegmatite: 1. textural variations across the pegmatite, i.e. grain size changes, 2. the evolution of the pegmatite from an igneous (border and wall zones) to a hydrothermal system (core zone), 3. the presence of beryl in the core zone only, and 4. the absence of garnet from the wall zone, where the disappearance of garnet defines the border-wall zone boundary.

All models assume the following: 1. The pegmatite evolves from a

Fig. 7.X Closed Model 1 (General case)

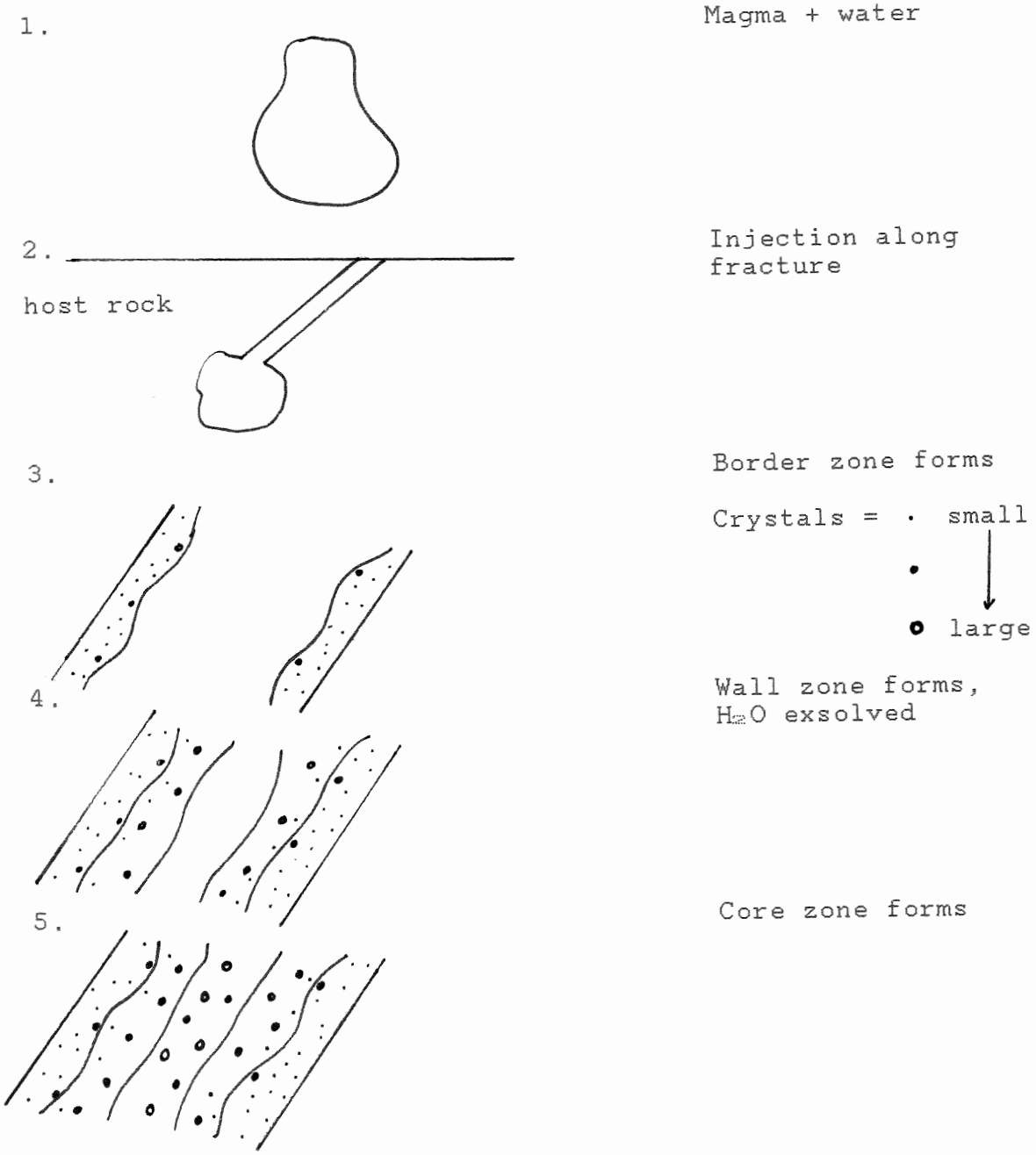

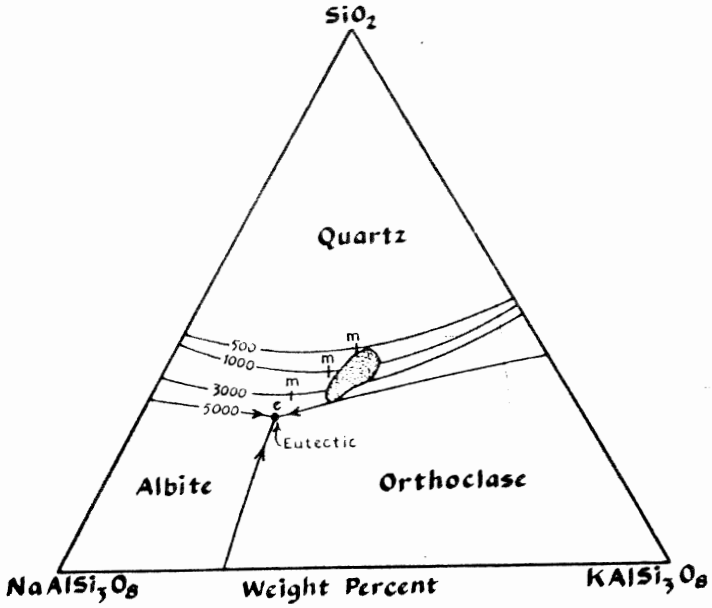

Fig. 7.4 The granite system, quartz-albite-orthoclase. The quartz-feldspar boundary and temperature minimum, m, is shown for 0.5, 1, 3, and 5 kilobars water pressure. Note that at 5 kilobars the temperature minimum becomes a eutectic and a cotectic line separates the fields of the two feldspars. The average composition of granitic rocks containing 80 percent or more of the three end-member components is indicated by the irregular oval area with shading.

McBirney 1984

A similar situation may occur with garnet at one apex (e.g. garnet instead of quartz at the quartz apex), such that the eutectic (or cotectic) moves toward the garnet apex, and an original bulk composition at point "e" is no longer saturated with respect to garnet.

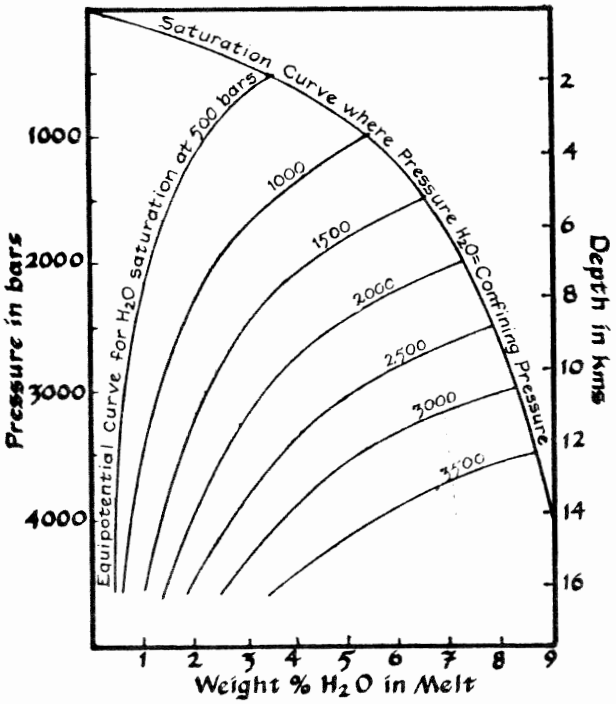

Fig. 7.5 The solubility of water in felsic magmas increases with increasing water pressure, but at constant water pressure, increasing load pressure on the magma decreases the solubility in the manner illustrated by the equipotential curves for different water pressures. Because water pressure increases more slowly with depth than load pressure in the magma, a vertical column of magma will tend to have a greater concentration of water at the top. (After G. C. Kennedy, 1955, *Geol. Soc. Amer. Spec. Paper 62*, 489–504.)

McBirney, 1984

water-rich magma injected along a fracture in the host rock, 2. The magma and hydrothermal phases remain saturated in quartz, K-feldspar, plagioclase, and muscovite throughout petrogenesis. The models presented below only serve as end members of petrogenesis, and may not apply to all pegmatites.

Model 1: Closed system

This model is closed in the sense that an initial pulse of magma is allowed to cool and evolve without modification by injection of any subsequent pulse. In this model, petrogenesis proceeds as follows:

1. A single pulse of H_2O-rich, but undersaturated, granitic magma injects along a fracture in the host rock. Expansion of this fracture results from injection of the magma (Jahns & Tuttle, 1963)(Fig. 7.X).
2. Crystallization begins, and relatively fine-grained crystals precipitate owing to the presence of the cooler host rock. Thus, the border zone forms.
3. As crystallization proceeds, so does the progressive enrichment of H_2O in the remaining magma (Jahns, 1982). The grain size of the pegmatite increases because crystallization now occurs farther from the cooler host rock. Thus, the wall zone forms.
4. The magma becomes over-saturated in H_2O, and as a result, the magma exsolves H_2O to create a hydrothermal system. This system allows very large crystals to precipitate, and thus forms the core zone.

Model 2: Open System

This system is open in that petrogenesis involves more than one pulse of magmatic origin, and the H_2O content of the magma increases with each successive pulse. Petrogenesis proceeds as outlined below.

1. An initial pulse of granitic magma injects along a fracture in the host rock, and starts to crystallize. Contact with the cooler host rock results in the formation of relatively fine-grained crystals. This first pulse forms the border zone (Fig. 7.X2).
2. A new pulse of a slightly different bulk composition injects, and slightly coarser crystals precipitate. This pulse forms the wall zone.
3. A third pulse, different in composition from the previous pulses, injects and forms the core zone.

In this model, the pulses may be of different compositions either because they come from different sources, or because the source of the pulses is constantly changing in composition (e.g. the late-stage differentiates of a larger igneous body).

Examination of Models: The Mechanisms

Both models account for the increase in grain size from the border to core, and thus satisfy the first criterion mentioned near the beginning of Section 7.3. The increase in grain size results from the slow cooling of the pegmatite, and from the presence of dissolved H_2O (border and wall zones) and exsolved H_2O (core zone). The H_2O facilitates high rates of diffusion, and hence permits the growth of very large crystals (Jahns, 1982). Model 2 is, however, flawed in that it should produce chilled contacts between the zones. Such chill margins are not observed in the main pegmatite.

Both models also account for the evolution of a hydrothermal system from an initially igneous system. In Model 1, this is accomplished by the exsolution of H_2O from a magmatic phase, resulting from a release of pressure as implied by the fluid inclusion data (Fig. 7.5)(Chapter 4). In Model 2,the last pulse must be oversaturated in H_2O to explain the

Fig. 7.X2 Open Model 2

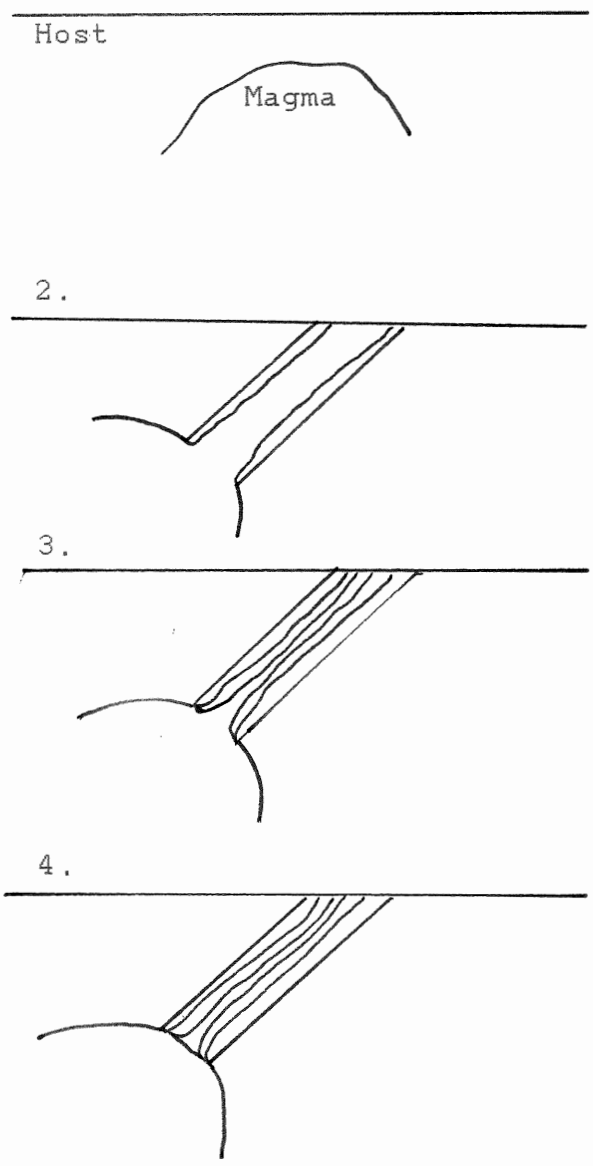

First pulse injected
Border zone forms

Second pulse injected
Wall zone forms

Last pulse injected
(hydrothermal)
Core zone forms

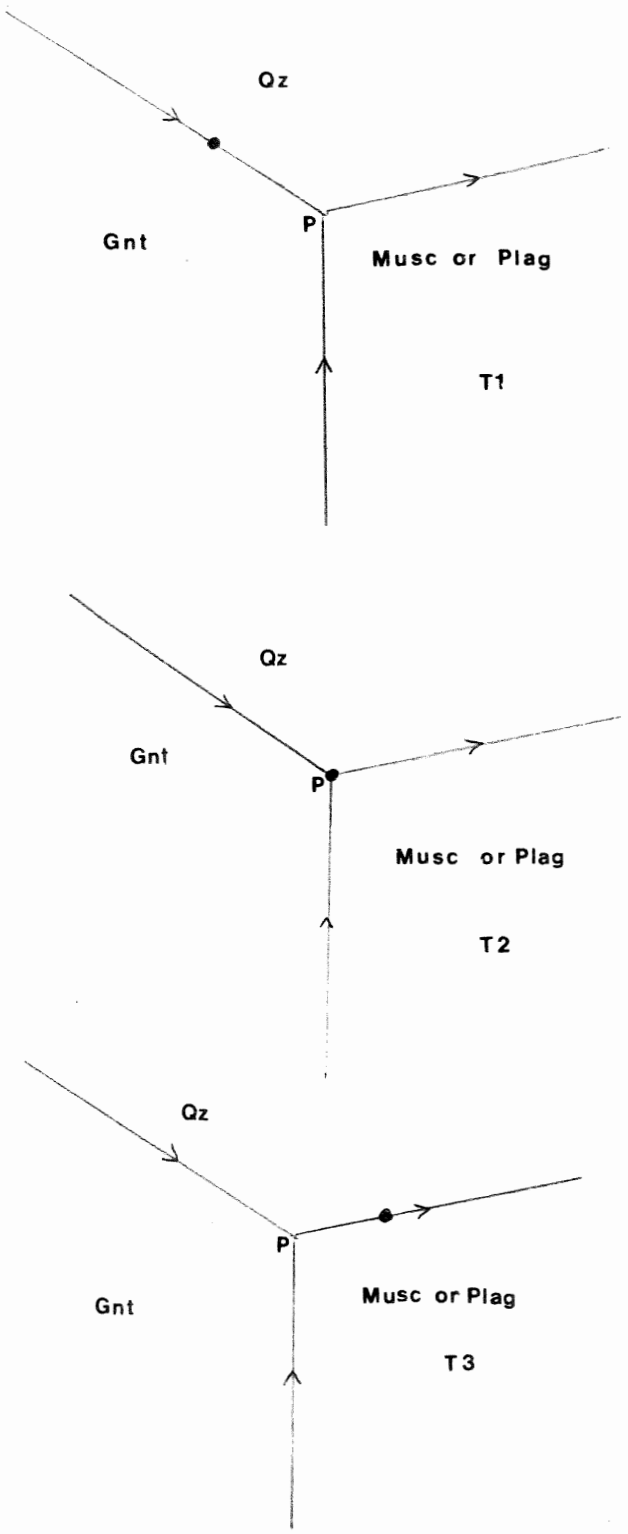

Fig. 7.6 Projection showing quartz, garnet, muscovite/plagioclase peritectic. Black dot represents the bulk composition at a given time, T1, T2 or T3. At T1 garnet + quartz crystallize, corresponding to the border zone. At T2 the system reaches the peritectic, and garnet + quartz + plagioclase/muscovite form, corresponding to the last part of the border zone. At T3 the system moves off the peritectic and garnet is no longer formed, corresponding to the wall zone.

igneous to hydrothermal transition.

A release of pressure during petrogenesis in Model 1 (and possibly in Model 2) explains the absence of garnet from the wall zone (Fig. 7.4). During the final stages of crystallization of the border zone, an abrupt, but not necessarily large pressure change would shift the cotectic lines of the system, such that the magma is no longer saturated in the garnet component. Model 1 does not account for the reappearance of garnet in the core zone. Model 2 accounts for the absence of garnet from the wall zone simply by assigning a bulk composition lacking a garnet component to the second pulse. By assigning a garnet component to the last pulse, Model 2 accounts for the presence of garnet in the core. Because of the fluid inclusion evidence, the pressure release hypothesis is more consistent with Model 1 than Model 2.

Fractionation through a peritectic point during petrogenesis may also explain the absence of garnet from the wall zone, in both models. As the wall zone starts to form, the system may pass through a peritectic point away from the garnet phase field (i.e. garnet no longer forms)(Fig. 7.6). This hypothesis does not explain the reappearance of garnet in the core zone.

The only reasonable way to form beryl in the core of the pegmatite in the case of Model 1 is to crystallize a melt initially relatively rich in Be. Beryllium is an incompatible element, and will reside in the melt or vapour phase over crystalline phases, until it is concentrated enough to form beryl (i.e. in the hydrothermal fluid of Model 1). In the case of Model 2, the last pulse is assigned an initial bulk composition with a beryl component, or the pulse may leach Be from another source as it passes through the host rock.

In general, neither model alone accounts for all the zonal features of the main pegmatite. Model 1 coupled with the pressure release hypothesis explains all of the zonal properties except the reappearance of garnet in the core zone. If the system changed from closed to open some time during the formation of the core zone, then the presence of garnet in the core zone is explained. Model 2 accounts for the chemical zonation of the pegmatite better than Model 1, but Model 2 does not agree well with the textural observations. Thus, the petrogenesis of the pegmatite may be best explained by the combination of Models 1 and 2, accompanied by a pressure release or fractionation through a peritectic.

7.4 Suggestions for Further Work

Some of the following activities might further the exploration of the origins of the Port Mouton pluton and associated pegmatites:

1. Construct a more complete trace element profile across the Wickwire pegmatite.

2. Survey all of the major zoned, beryl-bearing pegmatites in the pluton.

3. Make a more complete fluid inclusion study of the Wickwire and other zoned pegmatites.

4. Compare the properties of the zoned and unzoned pegmatites of the region to see if they are of different origins.

5. Compare the bulk compositions of the Meguma metasediments to that of the Wickwire pegmatite and associated host phases, to see if the Meguma is the protolith for these rocks.

6. Conduct a detailed age dating study of all the major zoned pegmatites to see if they formed contemporaneously or sporadically.

7. Perform a high-resolution, solid-state nuclear magnetic resonance study on the feldspars to discover their cooling histories.

Appendix A

Fluid Inclusions

Fluid inclusion theory is based on the fact that crystals growing from a fluid medium will commonly trap small pockets or bubbles of the fluid as they grow, owing to the cohesive forces acting between the bubble of fluid and the growing crystal face. These pockets of fluid are commonly composed of a homogeneous solution of gases, salts and liquid water. As the crystal and trapped inclusions cool, the components dissolved in the water will decrease in solubility and form vapour bubbles in the case of exsolved gases, or crystals in the case of precipitated salts(e.g. halides, silicates). The temperature at which these phases formed one homogeneous phase, an approximation of the temperature of crystallization of the mineral involved, can be determined by heating the cooled inclusion to a point where the phases are homogeneous once again.

By freezing the inclusion and observing the behaviour of the liquid and vapour parts of the inclusion and using the equations below, one can determine the salinity (NaCl content) of the fluid, telling something about the composition of the fluid from which the mineral crystallized.

Eqn 1 $W=1.76958\ \Theta -4.238^{-2}\ \Theta + 5.2778^{-4}\ \Theta$

Eqn 2 $\Theta= .581855W + 3.48896^{-3}W + 4.314^{-4}W$ (Roedder,1984)

W=salinity in weight percent, Θ=depression of freezing point

This type of work is done using a special microscope and stage enabling the investigator to heat the inclusion using an electrically resistant coil, and to freeze the inclusion using liquid nitrogen-cooled, inert gases.

Appendix B

X-ray Diffraction

In the technique of powder X-ray diffraction, a sample of pulverised mineral is placed inside a metal chamber and bombarded by X radiation of a single wavelength, and the outcoming reflected and diffracted X-rays are counted by a sensitive detector. Because the atoms in a mineral are arranged in a symmetrical, repeating, three-dimensional pattern, and the distances between the planes of atoms are on the order of the wavelength of X-rays, one can use X-rays to discover the atomic structure of a mineral. Under favorable conditions the electrons orbitting an atom in the crystal lattice will scatter an incident X-ray beam in a coherent manner, such that in certain directions the scattering of X-rays from millions of atoms in the crystal will be in phase simultaneously.

These directions are easily detected by the detector seeing an intense beam at a given angle of diffraction corresponding to a plane of atoms. The in-phase diffraction of X-rays is governed by the equation $n\lambda = 2d\sin\Theta$, where n is an integer(generally 1), λ is the wavelength of the incident wavelength, Θ is the angle between a plane of atoms and the incident X-rays, and d is the distance between planes of atoms. Because there is only one Θ angle at which the reflected rays are in phase for a given d and the rays interfere destructively at other angles, the detector will register an intense peak when these conditions are met. Thus, if one knows the wavelength and reflection angles for a given peak, one may calculate the d-spacing, and hence the lattice structure of a mineral, and assign unique peaks and intensities to given crystallographic orientations of the crystal.

Appendix C

X-ray Fluoresence

X-ray fluorescence techniques are used to determine the concentration of elements within a mineral to the ppm level. This technique is used to discover the chemical composition of a given mineral, and is commonly used for minerals with rare earths, because REEs are difficult to analyse conventionally owing to their chemical similarities. In this method, a powdered sample is bombarded with a spectrum of X-radiation, and each element fluoresces at a given intensity and wavelength in response to a given wavelength of X-radiation within the spectrum. In general, the amount of fluorescence from a given element in a sample is proportional to the amount of that element in the sample. The intensity of the fluorescence is not commonly linear with respect to concentration owing to self-fluorescence and self-absorption of X-rays, but these effects can be calibrated and effectively eliminated.

This method has two basic variations, namely wavelength and energy dispersion. In the first method, the wavelengths at which a given element fluoresces are measured and the intensities are compared to some standard to calculate the concentration of a given element. In the second method, the amount of energy coming from the irradiated sample is counted for given energy increments corresponding to different quantum energy levels within an atom. In this manner, a unique energy spectrum for each element in a mineral or rock is constructed, and the intensity of the energy peaks corresponds to the amount of an element in the sample. The energy dispersion method is by far the easier method to calibrate, and is more accurate than wavelength dispersion.

Appendix D

Electron Microprobe Analysis

This type of analysis is used to obtain detailed chemical analyses of individual mineral grains, and can be used to detect elements at the 50-100 ppm level in a given mineral. Microprobe analysis is based on the principle that given elements within a mineral will emit characteristic X-rays when bombarded by high-energy electrons. One can measure the emitted X-rays from an irradiated sample and identify the elements and their concentrations from the characteristic wavelengths(or energies) and intensities of the emissions relative to some internal standard, respectively.

The microprobe consists of a scanning electron microscope and several X-ray spectrometers, and some kind of electron-focusing device capable of adjusting the electron beam onto the surface of a sample. The electrons are accelerated through an electrical potential sufficient to give them enough energy to cause emission of X-rays from the specimens to be analyzed. The emitted X-rays can be analyzed either on the basis of wavelength or energy. With wavelength dispersive spectrometers(WDS) the emitted X-rays are dispersed by a curved crystal or diffraction grating such that the Bragg equation is satisfied($N = 2d\sin\theta$), and the various elements are mapped on the basis of their characteristic X radiation. In energy dispersive spectrometry(EDS), the emitted X-rays are measured on the basis of their energies, and radiation from all the elements is detected simultaneously and sorted electronically. Samples to be analyzed are finely polished and coated in carbon to allow the conduction of electrons away from the grain being analyzed. One can use probe analyses to obtain the stoichiometry of a given mineral.

References

Cameron E.N., Jahns R.H., McNair A., Page L.R. 1949. Internal structure of granitic pegmatites. Econ. Geol. Monogr. 2:1-115

Cerny P. ed. 1982. Anatomy and classification of granitic pegmatites, in Short Course In Granitic Pegmatites In Science And Industry. MAC Short Course 8:4, 5, 8, 20, 22-3, 30.

Cerny P. ed. 1982. Petrogenesis of granitic pegmatites, in Short Course In Granitic pegmatites In Science And Industry. MAC Short Course 8:405-450.

Clarke D.B., Muecke G.K. 1980. Halifax '80. GAC-MAC Field Trip Guidebook 21: Igneous and Metamorphic Geology of Southern Nova Scotia. Dalhousie University. p.48-71.

Douma S. 1988. The Mineralogy, Petrology, and Geochemistry of the Port Mouton Pluton, Nova Scotia, Canada. Master's Thesis, Dalhousie University.(in press)

Ginsburg A.I., Timofeyev I.N., Feldman L.G. 1979. Principles of geology in granitic pegmatites, in Short Course In Granitic Pegmatites In Science And Industry, P.Cerny ed., p.1-39.

Guilbert J.M., Park C.F. 1986. The Geology of Ore Deposits. W.H. Freeman & Co., U.S.A.. p.487, 489, 491, 497, 500-4.

Jahns R.H. 1953. The Genesis of Pegmatites. Am. Min. 38:563-598.

Jahns R.H. 1982. Internal Evolution of Pegmatitic Bodies, in Short Course In Granitic Pegmatites In Science And Industry, P.Cerny ed., p.293-318.

Jahns R.H., Tuttle O.F. 1963. Layered Pegmatite-Aplite Intrusives. Min. Soc. Am. Special Paper 1:78-92.

Jahns R.H., Burnham C.W. 1969. Experimental Studies of Pegmatite Genesis. 1. A Model for the Derivation and Crystallization of Granitic Pegmatites. Econ. Geol. 64:843-864.

Kent G.R. 1959. On four pegmatites in southwestern Nova Scotia. Master's Thesis, Dalhousie University. 74 pp.

Keppie J.D. 1979. Geological Map of Nova Scotia, 1:500,000.

Keppie J.D., Smith L. 1978. Report 78-4 Compilation of Isotopic Age Dates of Nova Scotia, Reference map 20P.

Marmo V. 1971. Granite Petrology and the Granite Problem. Elsevier Ltd., N.Y. p.25-30.

Martin R.F. 1982. Quartz and the Feldspars, in Short Course In Granitic Pegmatites In Science And Industry, P.Cerny ed., p.41-57.

McBirney A.R. 1984. Igneous Petrology. Freeman, Cooper & Co., U.S.A. p.351-373.

Raguin E. 1965. Geology of Granite. J.Wiley & Sons Ltd., N.Y. p.137-158.

Roedder E. 1984. Fluid Inclusions. MSA Reviews in Mineralogy 12:1-10, 251-304.

Simmons W.B., Lee M.T., Brewster R.H. 1987. Geochemistry and evolution of the South Platte granite-pegmatite system, Jefferson County, Colorado. Geoch. Cosmoch. Acta 51:455-472.

Smith D. ed., 1981. The Cambridge Encyclopedia of Earth Sciences. Prentice-Hall, Canada. p.60.

Varlamoff N. 1961. Relations spatiales entre les pegmatites et les granites en Afrique centrale et a Madagascar. Bull. Soc. Geol. France 7:711-722.

Winkler H.G.F. 1974. Petrogenesis of Metamorphic Rocks. Springer-Verlag, N.Y.. p.271-306.